© 2021. Published by The Company of Biologists Ltd | Development (2021) 148, dev194175. doi:10.1242/dev.194175

RESEARCH ARTICLE

Ciliopathic micrognathia is caused by aberrant skeletal differentiation and remodeling

Christian Louis Bonatto Paese[1,2], Evan C. Brooks[1,2], Megan Aarnio-Peterson[1,2,*] and Samantha A. Brugmann[1,2,3,‡]

ABSTRACT

Ciliopathies represent a growing class of diseases caused by defects in microtubule-based organelles called primary cilia. Approximately 30% of ciliopathies are characterized by craniofacial phenotypes such as craniosynostosis, cleft lip/palate and micrognathia. Patients with ciliopathic micrognathia experience a particular set of difficulties, including impaired feeding and breathing, and have extremely limited treatment options. To understand the cellular and molecular basis for ciliopathic micrognathia, we used the *talpid*^{2} (*ta*^{2}), a bona fide avian model for the human ciliopathy oral-facial-digital syndrome subtype 14. Histological analyses revealed that the onset of ciliopathic micrognathia in *ta*^{2} embryos occurred at the earliest stages of mandibular development. Neural crest-derived skeletal progenitor cells were particularly sensitive to a ciliopathic insult, undergoing unchecked passage through the cell cycle and subsequent increased proliferation. Furthermore, whereas neural crest-derived skeletal differentiation was initiated, osteoblast maturation failed to progress to completion. Additional molecular analyses revealed that an imbalance in the ratio of bone deposition and resorption also contributed to ciliopathic micrognathia in *ta*^{2} embryos. Thus, our results suggest that ciliopathic micrognathia is a consequence of multiple aberrant cellular processes necessary for skeletal development, and provide potential avenues for future therapeutic treatments.

KEY WORDS: Primary cilia, Ciliopathies, C2CD3, Micrognathia, Skeletal differentiation, Osteoblast, Bone remodeling, *talpid*^{2}, Chicken

INTRODUCTION

Primary cilia are ubiquitous microtubule-based organelles that serve as signaling hubs for multiple molecular signaling pathways (Goetz and Anderson, 2010). Disruptions in the structure or function of primary cilia result in a class of disorders known as ciliopathies. Clinically, ciliopathies commonly present with a range of phenotypes including polydactyly, situs inversus, retinitis pigmentosa and renal cystic disease (Baker and Beales, 2009). Approximately 30% of all ciliopathies can be classified as craniofacial ciliopathies owing to the craniofacial complex being the primary organ system affected (Zaghloul and Brugmann, 2011). Craniofacial ciliopathies are characterized by the common presentation of several phenotypes including cleft palate, craniosynostosis and micrognathia (Schock and Brugmann, 2017). Although some progress has been made towards understanding the pathologies associated with craniofacial ciliopathies (Cela et al., 2018; Chang et al., 2016a; Chang et al., 2014; Kawasaki et al., 2017; Millington et al., 2017; Schock et al., 2015; Tian et al., 2017; Watanabe et al., 2019), the cellular and molecular etiologies of ciliopathic craniofacial skeletal anomalies remain unclear.

Development of the mandible begins with the generation of cranial neural crest cells (NCCs) from the rostral neural tube. A subset of Hox-negative NCCs migrate from the dorsal neural tube into the first branchial arch where they proliferate and populate the mandibular prominence (MNP) (Couly et al., 1996; Kontges and Lumsden, 1996). After initial formation and patterning of the MNP, NCCs begin to differentiate into skeletal derivatives. A subset of NCCs condense and differentiate into chondrocytes to form a bilateral cartilaginous structure called Meckel's cartilage. Meckel's cartilage serves as a template for proper growth of the mandible, but it is not necessary for mandibular bone development (Mori-Akiyama et al., 2003). Other NCCs in the MNP undergo intramembranous ossification, in which NCCs condense and directly differentiate into osteoblasts. During intramembranous ossification, osteoblast differentiation is initiated when distal-less homeobox 5 (*DLX5*) induces the expression of runt-related transcription factor 2 (*RUNX2*), the master transcriptional regulator of bone development (Holleville et al., 2007; Lee et al., 2003). *RUNX2*+ NCCs differentiate into osteoblasts and secrete a specialized extracellular matrix called osteoid tissue. Osteoblasts embedded within the osteoid mature into osteocytes (reviewed by Franz-Odendaal, 2011).

After bone deposition, the developing mandible begins to take its characteristic shape via bone remodeling. Within the craniofacial skeleton, both mesoderm-derived osteoclasts and neural crest-derived osteocytes contribute to bone resorption via the secretion of tartrate-resistant acid phosphatase (TRAP) (Minkin, 1982; Qing et al., 2012; Tang et al., 2012), osteoclast-specific matrix metalloproteinase 9 (*MMP9*) (Engsig et al., 2000; Reponen et al., 1994), or osteocyte-specific matrix metalloproteinase 13 (*MMP13*) (Behonick et al., 2007; Johansson et al., 1997). TRAP is secreted into the bony matrix where it dephosphorylates the structural phosphoproteins osteopontin and bone sialoprotein (Ek-Rylander et al., 1994), whereas matrix metalloproteinases (MMPs) enzymatically degrade extracellular matrix components such as collagen and elastin to remodel tissues (reviewed by Cui et al., 2017). Levels of bone resorption are inversely proportional to jaw size and play an important role in determining overall mandibular size between and among species (Ealba et al., 2015). Despite numerous studies demonstrating that ciliary dysfunction leads to

[1]Division of Developmental Biology, Department of Pediatrics Cincinnati Children's Hospital Medical Center, Cincinnati, OH 45229, USA. [2]Division of Plastic Surgery, Department of Surgery, Cincinnati Children's Hospital Medical Center, Cincinnati, OH 45229, USA. [3]Shriners Children's Hospital, Cincinnati, OH 45229, USA.
*Present address: Sangamo Therapeutics, Brisbane, CA, USA.

‡Author for correspondence (samantha.brugmann@cchmc.org)

C.L.B.P., 0000-0001-5992-5209; E.C.B., 0000-0003-4895-8296; S.A.B., 0000-0002-6860-6450

Handling editor: Patrick Tam
Received 19 June 2020; Accepted 13 January 2021

Development (2021) 148, dev194175. doi:10.1242/dev.194175

micrognathia (Adel Al-Lami et al., 2016; Brugmann et al., 2010; Cela et al., 2018; Gray et al., 2009; Kitamura et al., 2020; Kolpakova-Hart et al., 2007; Zhang et al., 2011), whether or how loss of ciliary function affects bone resorption has yet to be described.

Owing to ample *in ovo* accessibility of NCCs and conserved organization of facial prominences, avian embryos have long been used to study craniofacial development (reviewed by Schock et al., 2016). Improved genome sequencing coupled with the existence of naturally occurring avian mutants have recently allowed researchers to make significant advances in understanding the etiology of developmental disorders using an avian model system. Perhaps the most used mutant avian lines have been those of the *talpid* family (Abbott et al., 1959, 1960; Ede and Kelly, 1964a,b). *talpid*^{2} (*ta*^{2}) is a naturally occurring avian mutant that is characterized by its striking presentation of polydactyly and craniofacial phenotypes (Abbott et al., 1959, 1960; Brugmann et al., 2010; Chang et al., 2014; Dvorak and Fallon, 1992; Muñoz-Sanjuán et al., 2001; Schneider et al., 1999). Our previous studies revealed that the causative mutation in the *ta*^{2} was a 19 bp deletion in C2 calcium-dependent domain containing 3 (*C2CD3*) (Chang et al., 2014), a distal centriolar protein-coding gene required for ciliogenesis (Hoover et al., 2008; Ye et al., 2014). Impaired C2CD3-dependent ciliogenesis in the *ta*^{2} results in facial clefting, ectopic archosaurian-like first generation teeth, hypo- or aglossia and micrognathia (Chang et al., 2014; Chang et al., 2016b; Harris et al., 2006; Muñoz-Sanjuán et al., 2001; Schock et al., 2015). Genetic, molecular and bioinformatic data from these studies determined that *ta*^{2} was a bona fide model for the human craniofacial ciliopathy, oral-facial-digital syndrome 14 (OFD14) (Schock et al., 2015). Although micrognathia is a common and severe craniofacial phenotype associated with OFD14 (Boczek et al., 2018; Cortés et al., 2016; Thauvin-Robinet et al., 2014), the molecular and cellular etiology of micrognathia in OFD14 patients and in *ta*^{2} embryos has yet to be explored.

In this study, we present the first in-depth analysis of the onset of ciliopathic micrognathia using the *ta*^{2} model. Our data demonstrate that, although there is an expansion of the SOX9+ osteochondroprogenitor population in the *ta*^{2}, osteoprogenitors undergo precocious and incomplete differentiation, resulting in a reduced number of mature osteoblasts. Furthermore, analysis of bone remodeling markers demonstrated that there is increased bone resorption in the *ta*^{2} mandible. Thus, our data suggest that ciliopathic micrognathia is due to the combinatorial effect of aberrant skeletal differentiation and remodeling.

RESULTS

ta^2 embryos present with micrognathia and dysmorphic skeletal elements

To understand the etiology of ciliopathic micrognathia, we first characterized the onset of micrognathia in *ta*^{2} embryos. The mandibular skeleton was first detectable via Alizarin Red staining at Hamburger-Hamilton stage (HH) 36. At this stage, skeletal elements that form the mandible, including the angular, dentary, splenial and surangular bones, were visible (Fig. 1A,A′). Relative to controls, Alizarin Red staining of HH36 *ta*^{2} mandibles revealed a reduction in calcified tissue (Fig. 1B,B′). Volumetric measurements of the *ta*^{2} angular, dentary, splenial and surangular bones confirmed a significant reduction in size relative to analogous control skeletal elements (Fig. 1C). *ta*^{2} embryos possessed a medial ectopic skeletal element adjacent to the splenial bone, as revealed via Alizarin Red (Fig. 1A′,B′) and micro-computed tomography (µCT) analysis (Fig. 1D-E′). Although the volume of the endogenous splenial bone alone was significantly reduced in *ta*^{2} embryos relative to controls, including the ectopic skeletal element in the analyses (the combined volume of the endogenous and ectopic *ta*^{2} splenial bone) eliminated a significant difference in volume (Fig. S1A). Whereas total mandibular volume and surface area were not significantly different at this stage (Fig. S1B,C), total length measurements revealed that the *ta*^{2} mandibles were significantly shorter than control mandibles at HH36 (Fig. 1F).

We further characterized mandibular development in control and *ta*^{2} embryos at HH39, the latest stage at which *ta*^{2} embryos can be consistently harvested before embryonic lethality (Abbott et al., 1959, 1960). At this stage, the developing *ta*^{2} mandible was reduced both in volume and surface area when compared with stage-matched control mandibles (Fig. 1G-J). µCT analysis confirmed the presence of an ectopic skeletal element medially adjacent to a severely reduced splenial bone in HH39 *ta*^{2} mandibles (Fig. 1H, yellow). These findings were further supported by whole-mount skeletal staining with Alizarin Red and Alcian Blue (Fig. S1D,E). Compared with HH39 control embryos, stage-matched *ta*^{2} mandibles were dysmorphic and possessed reduced Alizarin Red staining, indicative of decreased bone mineralization (Fig. S1E). Length measurements between controls and stage-matched *ta*^{2} mandibles confirmed that the micrognathia first observed at HH36 persisted in HH39 embryos (Fig. 1K). Although some elements in the mandible were dysplastic and thicker (a phenotype commonly seen in ciliopathic mutants; Brugmann et al., 2010; Cela et al., 2018; Kitamura et al., 2020; Kolpakova-Hart et al., 2007), the overall length of the mandible was reduced.

Avians have a distinct glossal apparatus that contains osteogenic and cartilaginous elements supported by the lingual process of the hyoid bone and rudimentary lingual muscles. Unlike the skeletal elements of the developing mandible that form through intramembranous ossification, the avian glossal and hyoid apparatus have skeletal elements that form through endochondral ossification, including the ceratobranchial bone (Lillie and Hamilton, 1952). To determine whether endochondral ossification was also affected in *ta*^{2} embryos, we examined the development of the ceratobranchial bone via Alizarin Red and Alcian Blue staining. Total length measurements revealed that the *ta*^{2} ceratobranchial was significantly reduced in size relative to controls (Fig. S1F-H). Although the hypoplastic ceratobranchial bones correlated with hypoglossia in *ta*^{2} embryos, it is interesting that hypo/aglossia was a defining phenotype of OFD14 patients despite humans lacking skeletal elements in the glossal apparatus (Boczek et al., 2018; Chang et al., 2014; Schock et al., 2015; Thauvin-Robinet et al., 2014). Thus, taken together, these analyses suggested that both endochondral and intramembranous ossification were impaired in *ta*^{2} mutants. Considering these findings, we next sought to examine the etiology of ciliopathic micrognathia by examining both cellular processes and molecular pathways required for mandibular development.

Aberrant Gli-mediated Hh activity in *ta*^{2} MNPs impacts cellular processes important for mandibular development

Although the mechanistic link between a number of signaling pathways and the cilium is not well understood, it is well-established that Gli-mediated Hedgehog (Hh) signaling requires primary cilia (Huangfu and Anderson, 2005; Huangfu et al., 2003). We previously reported that Hh signaling and Gli activity were impaired in *ta*^{2} embryos (Chang et al., 2014). Thus, to better understand the impact that aberrant Gli processing had on cellular processes essential for mandibular development, we examined genes associated with Gli-bound loci in the MNP, as determined by

Development (2021) 148, dev194175. doi:10.1242/dev.194175

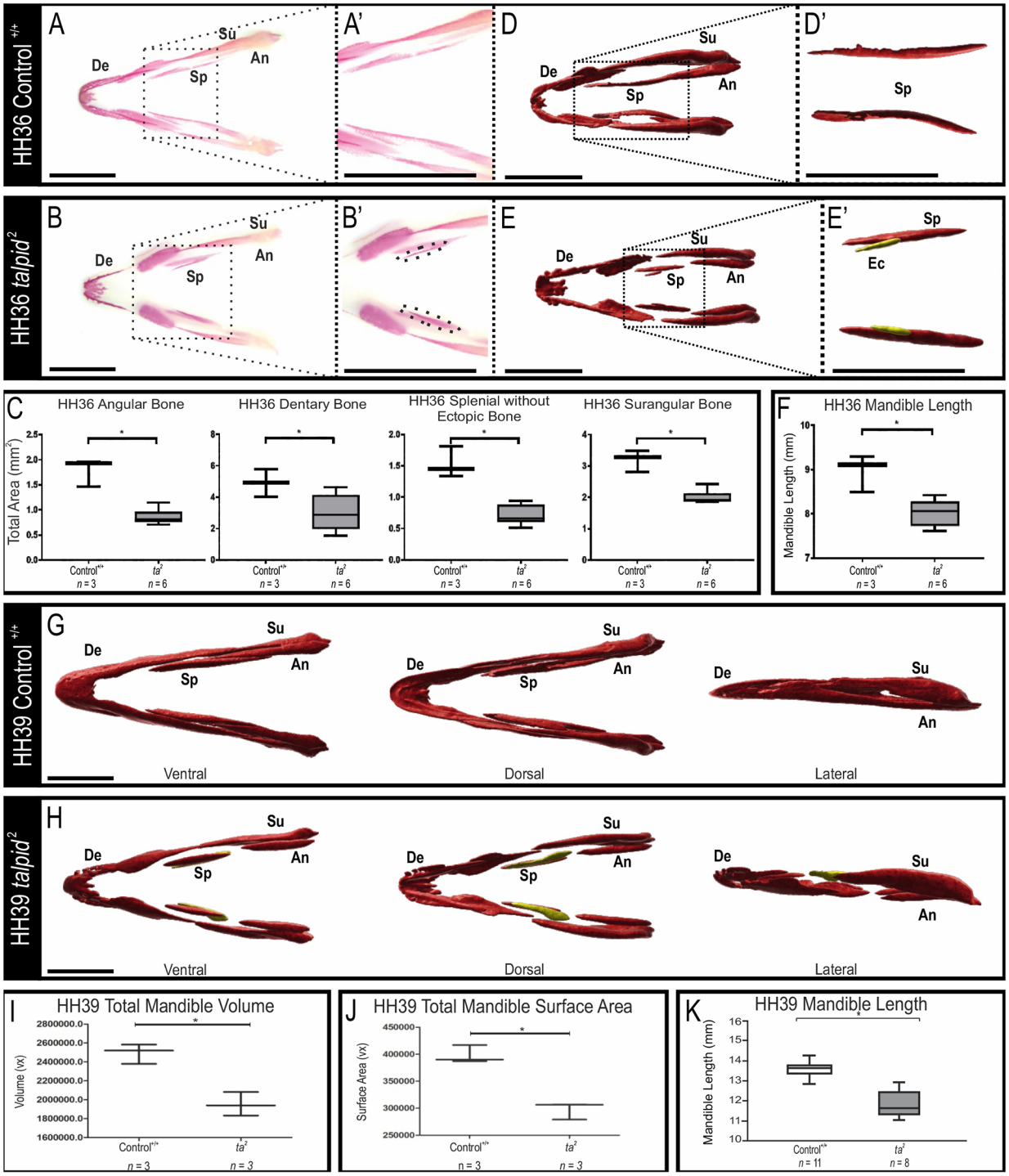

Fig. 1. Characterization of micrognathic onset in *ta²* embryos. (A-B′) Ventral views of Alizarin Red-stained HH36 control$^{+/+}$ (A; *n*=3) and *ta²* (B; *n*=6) mandibles, with insets (A′,B′) showing a higher magnification of the splenial bones. Dotted lines in B′ denote ectopic bone formation adjacent to the splenial bone. (C) Volumetric measurements of HH36 control$^{+/+}$ and *ta²* bones. (D-E′) Ventral views of µCT scans of HH36 control$^{+/+}$ (D) and *ta²* (E) mandibles. Insets (D′,E′) show higher magnification images of splenial bones (*n*=3 per group). For better visualization, the ectopic bone is pseudocolored in yellow. (F) Length measurements of HH36 control$^{+/+}$ and *ta²* mandibles. (G,H) µCT scans of HH39 control$^{+/+}$ (G) and *ta²* (H) mandibles (*n*=3 per group). (I,J) Total volume (I) and surface area (J), as measured in voxels (vx), of HH39 control$^{+/+}$ and *ta²* mandibles. (K) Length measurements of HH39 control$^{+/+}$ and *ta²* mandibles. An, angular; De, dentary; Ec, ectopic bone; Sp, splenial; Su, surangular. *P<0.05 (unpaired one-tailed Student's *t*-test). The middle of the box plots represent the median, and the whiskers demonstrate upper and lower quartiles (C,F,K). Data are mean±s.d. (I,J). Scale bars: 0.5 cm.

ChIP-seq (GSE146961) (Elliott et al., 2020; Lorberbaum et al., 2016) and cross-referenced this dataset against our previously published bulk RNA-seq dataset from control and *ta²* MNPs (GSE52757) (Chang et al., 2014). These analyses revealed a total of 1609 differentially expressed genes that were in close proximity to a Gli-bound locus, with an approximately equal number of target genes being either down- or upregulated (Fig. S2, Table S1). Gene ontology (GO) analysis for phenotypes associated with the 1609

Development (2021) 148, dev194175. doi:10.1242/dev.194175

differentially expressed presumptive Gli target genes in the *ta²* MNP tightly correlated with the observed phenotype and included 'abnormality of the mandible', 'abnormal jaw morphology' and 'abnormal facial shape'. Further GO analyses revealed the top biological processes impacted in the *ta²* MNP included 'positive regulation of cell cycle', 'ossification', 'regulation of microtubule cytoskeleton organization' and 'regulation of osteoblast differentiation' (Fig. 2). Based on these results we examined three cellular processes (cell-cycle progression, ossification and osteoblast differentiation) during mandibular development in *ta²* embryos in an attempt to better understand the molecular and cellular basis for ciliopathic micrognathia.

Cell cycle progression and cell proliferation are perturbed in the *ta²* mandibular prominence

Development of the mandibular skeleton initiates with an expansion of NCCs within the developing MNP. Ciliopathic mutants are particularly vulnerable to cell cycle disruptions as the centrioles required for ciliogenesis are the same organelles required for formation of the mitotic spindle. *In vitro* experiments have established that ciliogenesis is initiated at G1/G0. A mature/fully extended cilium is present at G0 and, upon cell cycle re-entry, microtubule stability is reduced, resulting in cilia disassembly (Fig. 3A) (Doxsey et al., 2005; Izawa et al., 2015; Kim et al., 2015; Kim and Tsiokas, 2011; Pugacheva et al., 2007; Tucker et al., 1979; Yeh et al., 2013). After disassembly, the basal body is released from its role in ciliogenesis, thereby freeing up centrioles to function in forming the mitotic spindle (Fig. 3A) (Kobayashi and Dynlacht, 2011; Nigg and Stearns, 2011). Our unbiased GO-analyses suggested that gene expression changes associated with 'positive regulation of the cell cycle' were enriched in *ta²* mutants. Given the impaired ciliogenesis in *ta²* mutants, we examined expression of genes associated with the G1/S checkpoint, a point at which ciliary retraction is necessary for cell passage into S phase and DNA replication (Tucker et al., 1979). We hypothesized that the lack of ciliogenesis in *ta²* mutants would correlate with unchecked progression from G1 to S. We first examined p21 expression: p21 arrests the passage from G1 to S phase if DNA damage or microtubular aberration is detected (Barr et al., 2017; el-Deiry et al., 1993). Thus, we hypothesized that reduced ciliogenesis in *ta²* mutants would correlate with reduced *p21* expression and unchecked passage through the cell cycle. qRT-PCR analysis revealed that *p21* expression was significantly decreased in the *ta²* MNPs relative to controls (Fig. 3B). We next examined expression of two positive G1/S regulators, cyclin D3 (*CCND3*) and ribosomal protein L23 (*RPL23*) (Bartkova et al., 1998; Qi et al., 2017). Expression of *CCND3* and *RPL23* were upregulated in *ta²* mutants by 28% and 43%, respectively (Fig. 3B). Together, these results suggest that impaired ciliogenesis in *ta²* mutants allows for unchecked progression through the G1/S cell cycle checkpoint.

Given these results, we next sought to determine whether and how unchecked cell cycle progression impacted cell proliferation rates in the osteochondroprogenitor population of the *ta²* MNP. Immunostaining for SOX9 (Ng et al., 1997) and phosphorylated histone H3 (PHH3) in HH26 control and *ta²* MNPs revealed that *ta²* MNPs had an increased SOX9+ population relative to control MNPs (Fig. 3C-G), despite there being no significant difference in total MNP area between control and *ta²* embryos (representing 21% of the total area in controls and 26.9% in *ta²* MNPs) (Fig. 3H). Double immunostaining for PHH3 and SOX9 further revealed that proliferation was significantly increased specifically within the SOX9+ population (Fig. 3I), whereas the proliferation was significantly decreased within the SOX9− mesenchyme (Fig. 3J). Cell death analysis, as assessed by cleaved caspase 3 (CC3) expression, revealed apoptosis was significantly decreased in *ta²* MNPs across both SOX9+ and SOX9− populations (Fig. S3A-F). Together, these data suggest that unchecked cell cycle progression leads to hyperproliferation specifically within SOX9+ osteochondroprogenitor cells in the *ta²* MNP. Previous studies have suggested that positively altering cell cycle progression in NCCs would result in premature formation of a mesenchymal condensation and cause the subsequent premature initiation of osteogenic differentiation (Hall et al., 2014). To further examine this possibility, we next analyzed the onset of osteogenic differentiation in *ta²* mutants.

Increased *RUNX2* expression correlates with an increased preosteoblast population in the *ta²* mandibular prominence

After sufficient proliferation, multipotent NCCs form a mesenchymal condensation and differentiate into several lineages, including the chondrogenic and osteogenic derivatives (Le Douarin, 1982). As expression for genes associated with the GO term 'regulation of osteoblast differentiation' were altered in *ta²* embryos, we sought to examine this process in a stepwise fashion. RUNX2 functions as the master transcriptional regulator for osteoblast differentiation, as increased *RUNX2* expression is required for the

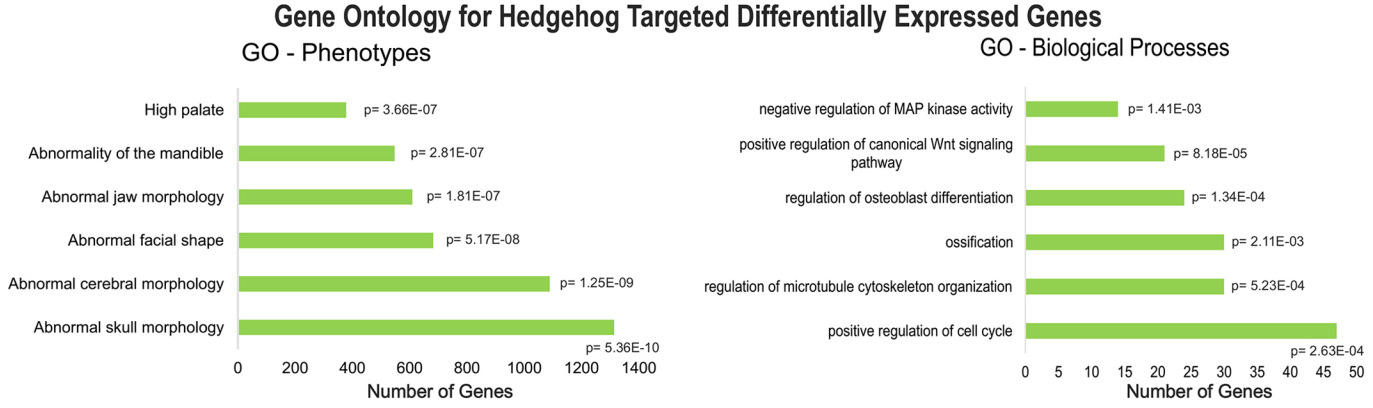

Fig. 2. Gene ontology analysis of Gli target genes demonstrate that cell cycle progression and osteogenesis are affected. Genes associated with Gli-bound loci were cross referenced against genes differentially expressed in the *ta²* MNP via RNA-seq. Graphs indicate the number of genes and *P*-values associated with GO Phenotypes and GO Biological Processes.

Development (2021) 148, dev194175. doi:10.1242/dev.194175

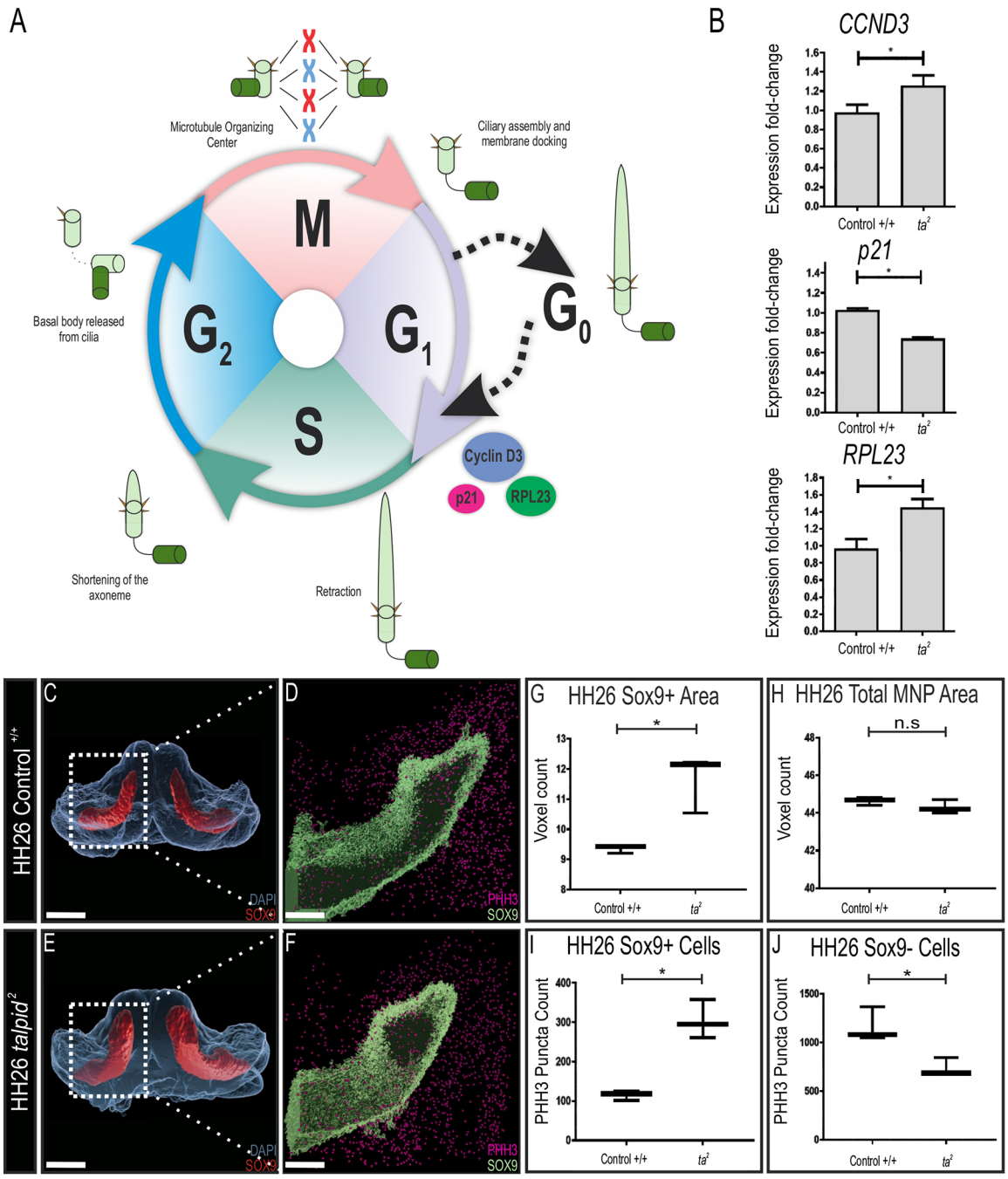

Fig. 3. Cell cycle progression and proliferation are impaired in NCC-derived skeletal progenitors within the *ta²* MNPs. (A) Schematic of cell cycle and primary cilia assembly. (B) qRT-PCR for *CCND3*, *p21* and *RPL23* in HH26 control$^{+/+}$ and *ta²* MNP (n=3 for control$^{+/+}$ and *ta²* samples). (C-F) Immunostaining for SOX9 (red) and DAPI (blue) surfaces in HH26 control$^{+/+}$ (C) and *ta²* (E) MNPs. Immunostaining for PHH3 (purple) and SOX9 (green) in HH26 control$^{+/+}$ (D) and *ta²* (F) MNPs. D,F show magnification of boxed areas in C,E, respectively. (G-J) Box plots show quantitative measurements of Sox9^{+} area, total area and PHH3 counts. (G) Voxel count of SOX9+ cells in HH26 control$^{+/+}$ and *ta²* MNPs (n=3). (H) Voxel count of DAPI surface in MNPs of HH26 control$^{+/+}$ and *ta²* (n=3). (I,J) PHH3+ (I) and PHH3– (J) puncta count in the SOX9+ cell population of control$^{+/+}$ and *ta²* MNPs (n=3). Data are mean±s.d. *P<0.05 (unpaired one-tailed Student's t-test). n.s, not significant. Plots reveal the upper and lower quartile. Median is represented by horizontal black line. Scale bars: 100 µm (C,E); 50 µm (D,F).

initial skeletal differentiation of NCCs into preosteoblasts (Komori et al., 1997; Otto et al., 1997). Once NCCs express *RUNX2*, they proceed down the osteoblast lineage (Fig. 4A) (Kobayashi et al., 2000). Previous studies have reported that *RUNX2* overexpression in earlier stages of development resulted in micrognathia in chick embryos (Hall et al., 2014). In the MNP, *RUNX2* expression is regulated both positively and negatively by additional transcription factors expressed in the developing MNP. DLX5 induces the expression of *RUNX2* (Holleville et al., 2007; Lee et al., 2003), whereas heart and neural crest derivatives expressed 2 (HAND2) inhibits *RUNX2* expression (Funato et al., 2009). To determine whether osteoblast differentiation was disrupted in *ta²* MNPs, we spatially and quantitatively examined expression of these genes. Both whole-mount and single molecule fluorescent *in situ* hybridization (Wang et al., 2012) revealed that *DLX5* expression was shifted distally around Meckel's cartilage in the HH29 *ta²*

Development (2021) 148, dev194175. doi:10.1242/dev.194175

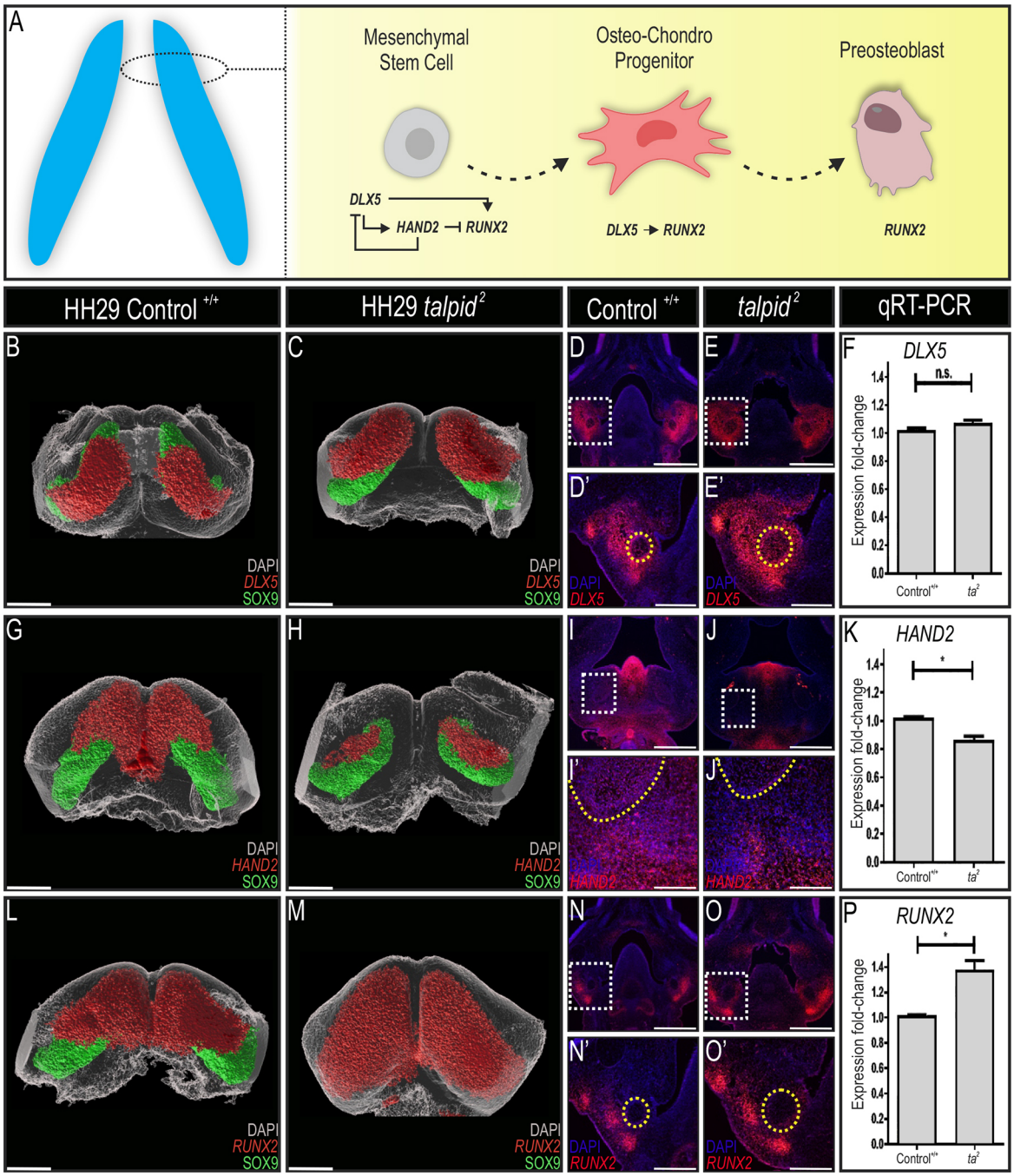

Fig. 4. Differentiation of NCC-derived osteochondroprogenitors is impaired in *ta²* MNPs. (A) Schematic demonstrating the osteochondroprogenitor gene regulatory network present in the developing MNP. (B,C) Whole-mount *DLX5 in situ* hybridization (red) in HH29 control$^{+/+}$ (B) and *ta²* (C) MNPs counterstained with SOX9 antibody (green). (D-E′) RNAscope *in situ* hybridization for *DLX5* in frontally sectioned HH29 control$^{+/+}$ (D) and *ta²* (E) heads, with higher magnifications of the Meckel's cartilage region in boxed areas shown in D′ and E′. (F) qRT-PCR for *DLX5* transcripts in HH29 control$^{+/+}$ and *ta²* MNPs (n=3). (G,H) Whole-mount *HAND2 in situ* hybridization (red) in HH29 control$^{+/+}$ (G) and *ta²* (H) MNPs counterstained with SOX9 antibody (green). Expression in control MNPs demonstrates ectodermal expression ventrally, as previously published. (I-J′) RNAscope *in situ* hybridization for *HAND2* in frontally sectioned HH29 control$^{+/+}$ (I) and *ta²* (J) heads, with higher magnification of boxed areas in I′ and J′. (K) qRT-PCR for *HAND2* transcripts in HH29 control$^{+/+}$ and *ta²* MNPs (n=3). (L,M) Whole-mount *RUNX2 in situ* hybridization in HH29 control$^{+/+}$ (L) and *ta²* (M) MNPs counterstained with SOX9 antibody (green). (N-O′) RNAscope *in situ* hybridization for *RUNX2* in frontally sectioned HH29 control$^{+/+}$ (N) and *ta²* (O) heads, with higher magnifications of boxed areas in N′ and O′. (P) qRT-PCR for *RUNX2* transcripts in HH29 control$^{+/+}$ and *ta²* MNPs (n=3). Dotted yellow lines in D′,E′,I′,J′,N′,O′ outline Meckel's cartilage. Data are mean±s.d. **P*<0.05 (unpaired one-tailed Student's *t*-test). n.s., not significant. Scale bars: 200 µm (B,C,G,H,L,M); 50 µm (D,E,I,J,N,O); 10 µm (D′,E′,N′,O′); 5 µm (I′,J′).

MNPs relative to controls (Fig. 4B-E′). Despite this spatial shift in expression, qRT-PCR analysis did not detect a significant change in the level of *DLX5* expression in the *ta²* MNP (Fig. 4F). Conversely, *HAND2* expression was lost distally and significantly decreased within the developing *ta²* MNP (Fig. 4G-K). Lastly, examination of *RUNX2* expression demonstrated a significant and robust proximal expansion in the developing *ta²* MNP (Fig. 4L-O′). This observation was confirmed quantitatively via qRT-PCR, which

Development (2021) 148, dev194175. doi:10.1242/dev.194175

revealed that *RUNX2* expression was significantly increased by 38% in the *ta*^{2} MNP (Fig. 4P). Sagittal *z*-stack projections of the MNP revealed that transcripts for all three genes were detected ventrally adjacent to the SOX9+ population (Fig. S4A-F; Movie 1). Together, these data suggest that excessive expression of *RUNX2*, correlated with the decreased expression of the negative regulator *HAND2*, resulted in ectopic production of pre-osteoblasts in the *ta*^{2} MNP.

Osteoblast maturation is impaired in *ta*^{2} mutants

Increased *RUNX2* expression could be indicative of increased bone deposition; however, in the *ta*^{2}, increased *RUNX2* expression accompanied a micrognathic phenotype. We hypothesized that, despite an expansion of pre-osteoblasts, transition towards a mature osteoblast was impaired in *ta*^{2} mandibles. Osteoblast maturation occurs in three stages. In the first stage, pre-osteoblasts proliferate and express collagen type 1 (COL1A1) protein. In the second stage, pre-osteoblasts exit the cell cycle and differentiate, while expressing alkaline phosphatase (ALPL) and COL1A1 (Rodrigues et al., 2012). In the last phase, mature osteoblasts express osteocalcin (OCN; also known as BGLAP), a protein that is essential for matrix mineralization (Fig. 5A) (reviewed by Rutkovskiy et al., 2016). First, to confirm the specificity of our reagents to delineate these

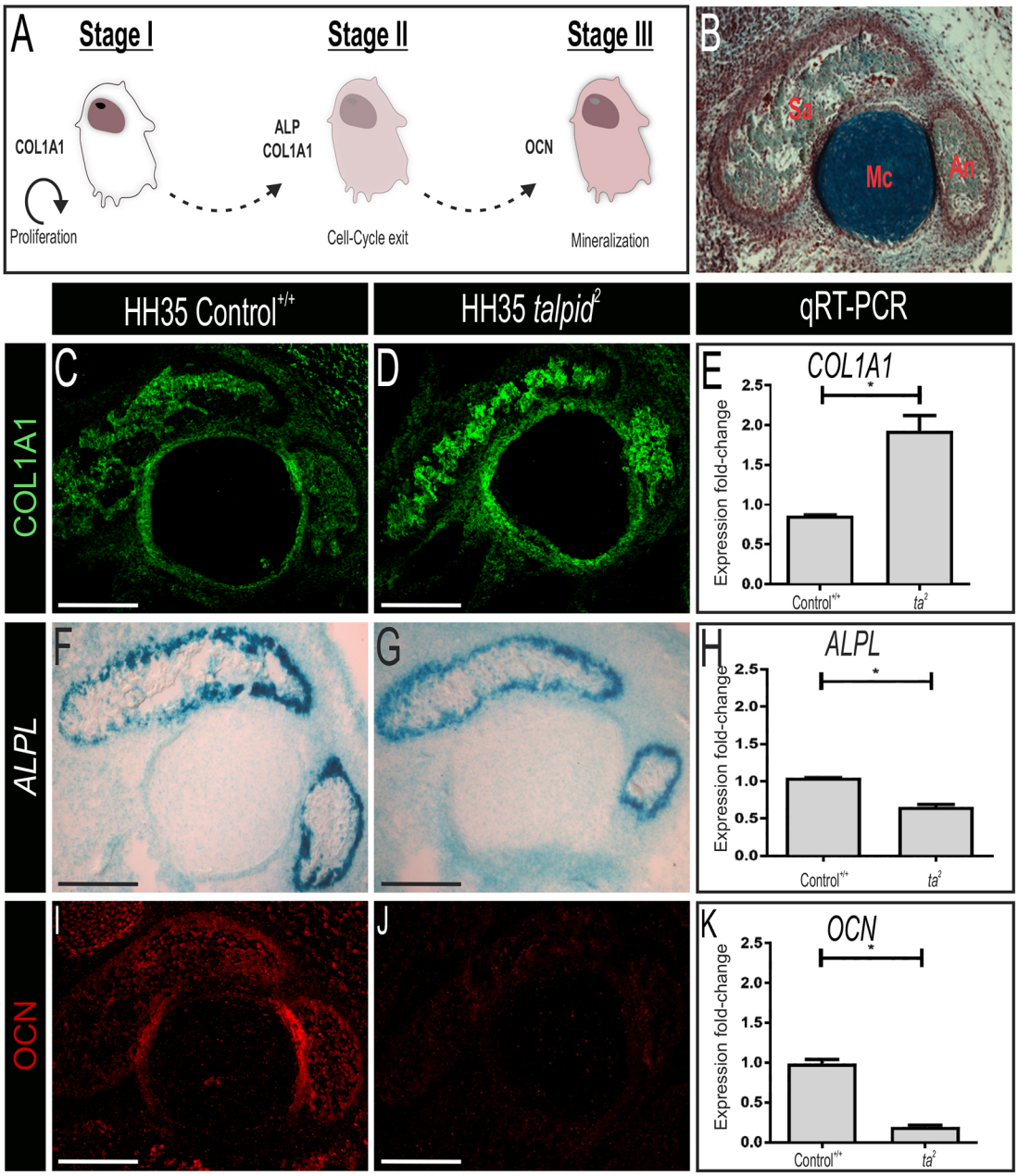

Fig. 5. Osteoblast maturation is impaired in *ta*^{2} mandibles. (A) Schematic denoting stages of osteoblast maturation. (B) Pentachrome staining of HH35 control$^{+/+}$ mandible for section visualization with the angular bone (An), Meckel's cartilage (Mc) and surangular bone (Sa) labeled for orientation. (C,D) Immunofluorescence staining on sections for COL1A1 in control$^{+/+}$ (C) and *ta*^{2} (D) mandibles at HH35. (E) Quantification of *COL1A1* transcripts by qRT-PCR in HH35 control$^{+/+}$ and *ta*^{2} mandibles (*n*=3). (F,G) RNAscope *in situ* hybridization staining for *ALPL* in HH35 control$^{+/+}$ (F) and *ta*^{2} (G) surangular sections denoted in blue (*n*=3). (H) Quantification of *ALPL* transcripts by qRT-PCR in HH35 control$^{+/+}$ and *ta*^{2} mandibles (*n*=3). (I,J) Immunofluorescence staining on sections for OCN in control$^{+/+}$ (I) and *ta*^{2} (J) mandibles at HH35. (K) Quantification of *OCN* transcripts by qRT-PCR in HH35 control$^{+/+}$ and *ta*^{2} mandibles (*n*=3). Data are mean±s.d. *P<0.05 (unpaired one-tailed Student's *t*-test). Scale bars: 100 µm (C,D,I,J); 80 µm (F,G).

Development (2021) 148, dev194175. doi:10.1242/dev.194175

stages of osteoblast maturation, we performed RNAscope *in situ* hybridization for *ALPL* and immunohistochemistry for COL1A1 and OCN on sagittal sections of an HH35 control femur (Fig. S5). We readily identified *ALPL*+ cells in the bony collar of the developing femur, COL1A1+ pre-osteoblasts within the extracellular matrix and OCN+ cells in the bony matrix (Fig. S5C-G). In frontal sections through the *ta*^{2} surangular bone (Fig. 5B), COL1A1 expression was increased relative to controls (Fig. 5C,D). qRT-PCR analysis supported this finding and revealed a significant, twofold upregulation in the expression of *COL1A1* (Fig. 5E). *ALPL* expression, which was localized to cortical surfaces of the developing skeletal elements in HH35 control mandibles, was reduced in *ta*^{2} mandibles (Fig. 5F,G). Quantification of *ALPL* transcripts in HH35 mandibles revealed a 35% downregulation in *ta*^{2} mandibles in comparison with control mandibles (Fig. 5H). Lastly, we analyzed the expression of OCN. OCN expression was reduced in the developing *ta*^{2} mandible when compared with controls (Fig. 5I,J). qRT-PCR analysis supported this finding and revealed that *OCN* expression was significantly reduced by ∼72% in *ta*^{2} mandibles relative to controls (Fig. 5K). Taken together, these results suggest that, despite an expansion of the pre-osteoblast population, osteoblast maturation was severely impaired. Thus, our data suggest that impaired osteoblast maturation and subsequently reduced bone deposition contributes to ciliopathic micrognathia.

Bone resorption is upregulated in *ta*^{2} mandibles

Several studies have reported that proper determination of jaw length requires regulated bone remodeling. Bone remodeling is a dynamic process that consists of resorption of bony matrix by osteoclasts and osteocytes and deposition of new bony matrix by osteoblasts. We next sought to determine whether aberrant bone remodeling also contributes to ciliopathic micrognathia, as it was previously reported that the amount of bone resorption was inversely proportional to jaw length in avian embryos (Ealba et al., 2015). To test the hypothesis that increased bone resorption contributes to ciliopathic micrognathia, we examined the expression of several markers for this process in sections through the HH39 surangular bone. We first assayed TRAP activity. When compared with controls, TRAP staining was increased in HH39 *ta*^{2} mandibles, indicative of increased bone resorption (Fig. 6A,B). We next examined expression of MMPs, a family of proteases necessary for osteoclast recruitment and solubilization of the osteoid during bone remodeling (reviewed by Cui et al., 2017). During mandibular remodeling, *MMP13* is expressed in NCC-derived osteoblasts and osteocytes (Behonick et al., 2007; Johansson et al., 1997). *In situ* hybridization and qRT-PCR revealed increased *MMP13* expression in the HH39 *ta*^{2} mandible when compared with controls (Fig. 6C,D). To confirm this result, we analyzed a second marker of bone resorption, secreted phosphoprotein 1 (SPP1). SPP1 is responsible for osteoclast adhesion and bone resorption across various species (Choi et al., 2008; Pinero et al., 1995). *SPP1* was more prominently expressed in the medullar region of the developing *ta*^{2} mandible relative to controls (Fig. 6E,F). These data were verified via qRT-PCR, revealing a significant twofold increase in both *MMP13* and *SPP1* expression in the *ta*^{2} mandibles relative to controls (Fig. 6G,H). Finally, we examined the ratio of receptor activator of NF-κB ligand (RANKL; TNFSF11) to osteoprotegerin (OPG; TNFRSF11B) expression. OPG protects bone from excessive resorption by binding to RANKL and preventing it from binding to its receptor, RANK (TNFRSF11A) (Fig. 6I). qRT-PCR analyses revealed that both *RANKL* and *OPG* expression were significantly increased in the developing *ta*^{2} mandible (Fig. 6J). Aberrant expression of both markers resulted in an increased ratio of RANKL/OPG expression (Fig. 6J), further suggesting that excessive bone resorption contributes to the onset of ciliopathic micrognathia in *ta*^{2} embryos.

Herein, we explored the etiology of ciliopathic micrognathia using the *ta*^{2} model as our guide. We found that, despite increased proliferation and expansion of osteochondroprogenitors and preosteoblast populations, osteoblast maturation and subsequent bone deposition was impaired in the *ta*^{2} mandible. Furthermore, excessive amounts of bone resorption were also detected following impaired bone deposition (Fig. 7). These studies are significant as they increase the understanding of the cellular processes and molecular pathways that can be targeted for future therapeutic approaches for ciliopathies.

DISCUSSION

Micrognathia is a significant biomedical burden present in almost 20% of ciliopathies (Schock and Brugmann, 2017). The predominant treatment for micrognathia is distraction osteogenesis, an invasive and traumatic procedure in which the mandible is cut and gradually separated to allow new bone growth until the mandible reaches a desired size (Ilizarov, 1988). To develop less invasive therapeutic options for ciliopathic micrognathia, it is important to gain a more extensive understanding of its etiology. Although studies have shown that loss of primary cilia leads to micrognathia, a thorough analysis of how the cellular and molecular mechanisms essential for mandibular development are impaired in ciliopathic mutants has yet to be described. To this end, we used the avian ciliopathic mutant *ta*^{2}, a bona fide model of the human ciliopathy OFD14, to investigate how ciliopathic micrognathia arose. Whereas the majority of ciliopathic studies use conditional knockout murine models, the naturally occurring *ta*^{2} model, in which the ciliopathic insult is ubiquitous throughout the organism, allowed for analyses more relevant to human ciliopathic conditions. Our previous data, together with that reported herein, revealed that loss of C2CD3-mediated ciliogenesis resulted in impaired Gli-mediated Hh signal transduction. Impaired Hh signaling (via direct or indirect mechanisms) resulted in unchecked cell cycle progression, subsequent increased proliferation of SOX9+ osteochondroprogenitors and impaired expression of gene regulatory networks necessary for the maturation of NCC-derived osteoblasts. Furthermore, excessive bone resorption was detected in *ta*^{2} mandibles later in development (Fig. 7A,B). To our knowledge, this work represents the first in-depth description of the etiology of ciliopathic micrognathia.

NCC-derived skeletal precursors are highly sensitive to ciliopathic insults

The cell cycle and ciliogenesis both require centriolar function and are thus inextricably linked. Previous studies solidified this relationship, reporting that knockdown of the ciliary protein IFT88 promoted cell cycle progression and proliferation (Robert et al., 2007). Furthermore, previous studies have also shown that cell cycle progression and the onset of osteogenesis are tightly correlated and autonomously controlled within NCCs (Hall et al., 2014). Our current study revealed that NCC-derived skeletal progenitors in the MNP were specifically affected, as seen by increased cell proliferation in the SOX9+ population of *ta*^{2} MNPs. Integrating these data with those previously reported (Ealba et al., 2015; Hall et al., 2014), we hypothesize that loss of cilia allows for the unchecked passage of NCCs in the MNP through the cell cycle, which subsequently results in premature formation of a mesenchymal condensation and early execution of the skeletal differentiation program. Although, our previous studies examining

Development (2021) 148, dev194175. doi:10.1242/dev.194175

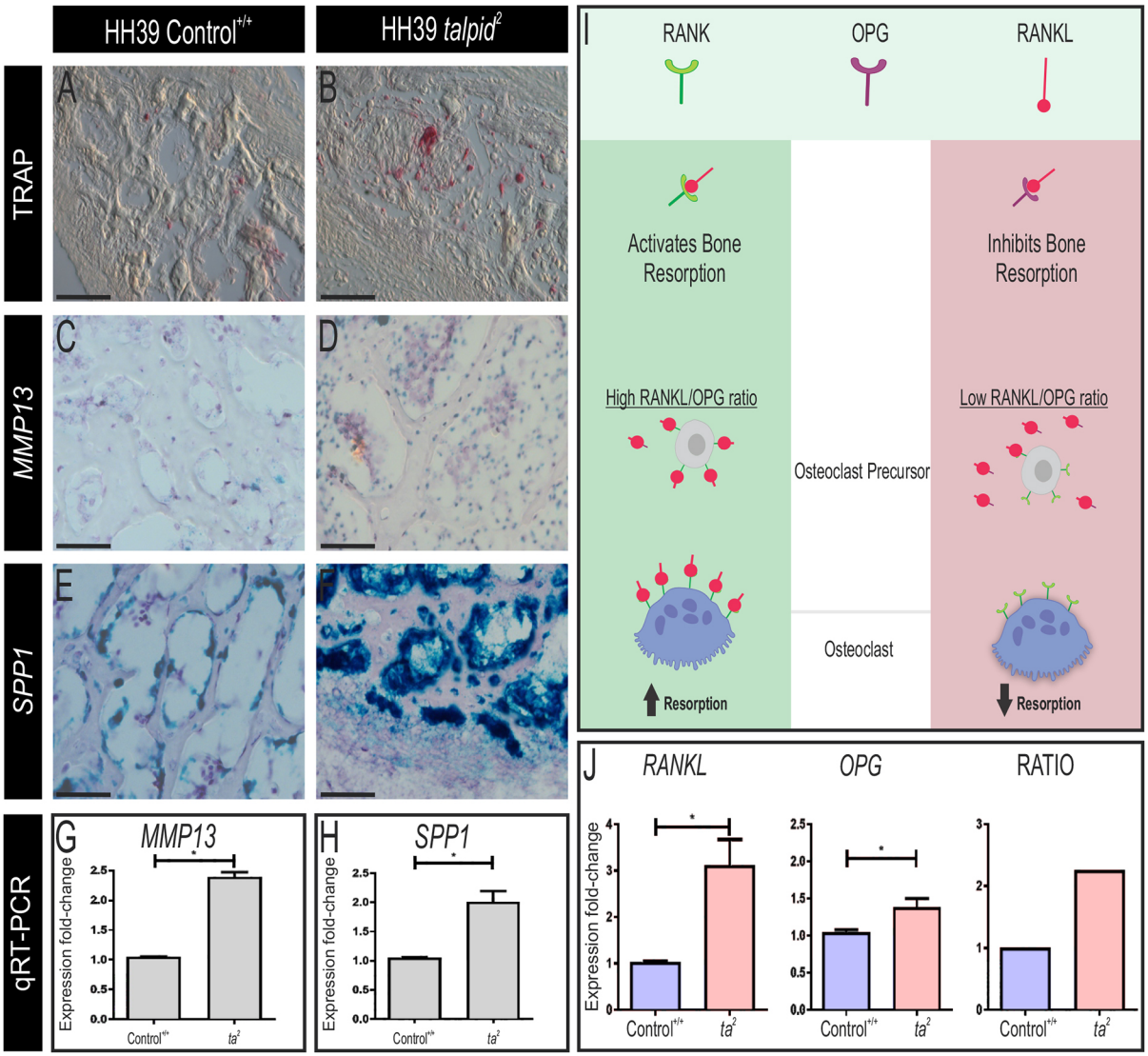

Fig. 6. Bone resorption is increased in *ta*^{2} mandibles. (A,B) TRAP staining in HH39 control$^{+/+}$ (A) and *ta*^{2} (B) mandibles (*n*=3). (C,D) RNAscope *in situ* hybridization for *MMP13* in HH39 control$^{+/+}$ (C) and *ta*^{2} (D) surangular sections (*n*=3). (E,F) RNAscope *in situ* hybridization staining for *SPP1* in HH39 control$^{+/+}$ (E) and *ta*^{2} (F) surangular sections (*n*=3). (G-H) qRT-PCR quantification of *MMP13* (G) and *SPP1* (H) transcripts in HH39 control$^{+/+}$ and *ta*^{2} mandibles (*n*=3). (I) Schematic of RANK/RANKL/OPG regulation of osteoclast-mediated bone resorption. (J) Quantification of *RANKL* and *OPG* expression and the *RANKL*/*OPG* ratio in HH39 control$^{+/+}$ and *ta*^{2} mandibles (*n*=3). Scale bars: 100 µm (A,B); 50 µm (C-F). Data are mean±s.d. **P*<0.05 (unpaired one-tailed Student's *t*-test).

cell proliferation in early, undifferentiated NCC populations of the frontonasal prominence did not reveal any alteration in proliferation rates between control and *ta*^{2} embryos (Schock et al., 2015), these data still beg the question: are NCC-derived skeletal progenitors more sensitive to a ciliopathic insult than other cell types?

There is some precedent for the idea of cell-specific sensitivities. Treacher-Collins syndrome (TCS) is a congenital craniofacial disorder characterized by hypoplasia of facial bones, high arched palate and ear defects. Seminal studies addressing the etiology of TCS determined that NCCs, owing to their high energetic demands as highly proliferative and migratory multipotent cells, were especially sensitive to deficient ribosome biogenesis and subsequent cellular stress (Dixon et al., 2006; Jones et al., 2008). Studies on various cell types are beginning to uncover a connection between the cilium and energy homeostasis (Arsov et al., 2006; Collin et al., 2005; Davenport et al., 2007; Marion et al., 2009; Pampliega et al., 2013; Tang et al., 2013). In addition, the process of osteogenic differentiation, and maturation of osteoblasts in particular, has a heavy requirement of oxidative phosphorylation and glycolysis (Guntur et al., 2014; Regan et al., 2014). Thus, the lack of primary cilia on skeletal progenitors could result in a similar type of cellular stress, preventing *ta*^{2} NCCs from executing proliferation and differentiation programs that allow for proper skeletogenesis in the developing MNP.

Disruptions in Gli-mediated cellular processes contribute to ciliopathic micrognathia

Gli transcription factors are post-translationally processed into functional activator (GliA) or repressor (GliR) isoforms at the primary cilium (Goetz and Anderson, 2010; Haycraft et al., 2005; Liu et al., 2005). Loss of functional Gli isoforms results in altered transcription of Hh pathway target genes (Chang et al., 2014). We have previously shown that all facial prominences of *ta*^{2} mutants have perturbed Gli processing and subsequent disruptions in Hh signal transduction (Chang et al., 2014). Here, we advanced our understanding of the molecular etiology of ciliopathic phenotypes

Development (2021) 148, dev194175. doi:10.1242/dev.194175

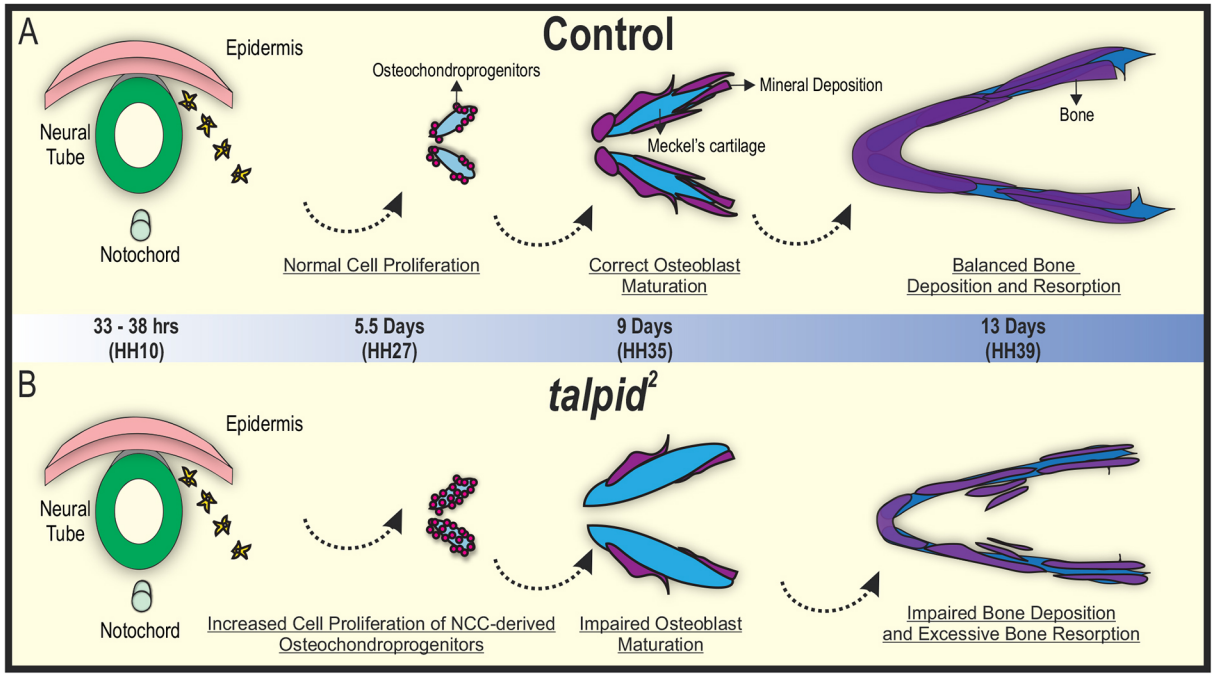

Fig. 7. Summary of mandibular development in control and *ta²* embryos. (A,B) Schematic of NCCs undergoing intramembranous ossification in control (A) and *ta²* (B) mandibles. In summary, NCCs migrate from the dorsal neural tube and populate the MNP. NCCs differentiate into osteochondroprogenitors at 5.5 days of development. In *ta²* MNPs, increased proliferation of NCC-derived osteochondroprogenitors coupled with aberrant expression of transcription factors necessary for skeletal differentiation results in the generation of osteoblasts that fail to fully mature, and a subsequent decrease in bone mineralization. Misregulation of these processes, together with excessive bone resorption, result in ciliopathic micrognathia.

by comparing Gli bound loci with genes that were differentially expressed in *ta²* MNPs. Our results suggested that loss of proper Gli-mediated transcription impacted several cellular processes necessary for mandibular development, including positive regulation of the cell cycle, ossification and osteoblast maturation. These data not only explain the phenotypic similarities frequently observed between Hh and ciliopathic mutants (Abzhanov et al., 2007; Billmyre and Klingensmith, 2015; Elliott et al., 2020; Jeong et al., 2004; Lenton et al., 2011; Xu et al., 2019), but also provide new insight into pathways that may be available for therapeutic intervention.

Although these data strongly suggest that impaired Gli-mediated Hh signaling is molecularly causal for the micrognathic phenotype, the exact molecular mechanisms by which this occurs remains unknown. For example, it is possible that the onset of micrognathia is due to a failure of Gli isoforms to directly regulate transcription of targets necessary for skeletal differentiation. Our GLI2 and GLI3 ChIP-seq data reveal Gli peaks near the transcriptional start site of *HAND2* and within the *RUNX2* locus (Elliott et al., 2020). It is also possible, however, that impaired ciliary-dependent Gli processing impairs the ability of Gli proteins to interact with skeletal transcription factors. GLI2 was reported to physically interact with RUNX2 to direct osteoblast differentiation (Shimoyama et al., 2007) and GLI3 was reported to utilize HAND2 as a co-factor to drive the mandibular patterning and osteogenic transcriptional programs (Elliott et al., 2020). Understanding the exact molecular mechanisms associated with ciliopathic phenotypes is the focus of our ongoing work.

Despite our focus on the Hh pathway, other signaling pathways, such as the Wnt, fibroblast growth factor (FGF), and bone morphogenetic protein (BMP) pathways, are also known to be involved in skeletal development (Jiang et al., 2014; Merrill et al., 2008; Mina et al., 2007); however, the mechanisms by which these pathways require cilia-dependent signaling transduction is less clear. The role of the cilium in canonical Wnt signaling has been heavily disputed. Initial studies demonstrated that numerous Wnt pathway components, such as inversin, Vangl2 and Apc, localized to the ciliary axoneme or basal body, suggesting a role for primary cilia in Wnt signal transduction (Morgan et al., 2002; Ross et al., 2005; Simons et al., 2005). Subsequent studies demonstrated that the cilium functions to repress Wnt signaling, as loss of cilia correlated with increased Wnt activity and Wnt target gene expression (Corbit et al., 2008; Lancaster et al., 2011). Concurrent studies in mice and zebrafish that lack various ciliary proteins retained normal levels of canonical and non-canonical Wnt signaling transduction (Huang and Schier, 2009; Ocbina et al., 2009). Further, in the NCC-derived facial mesenchyme, conditional loss of the ciliary protein Kif3a in NCCs did not appear to alter Wnt activity (Brugmann et al., 2010). Recently, it was found that deletion of Kif3a plays a role in Wnt signaling in a ciliary-independent fashion by activating the pathway in an autocrine manner (Kim et al., 2016). If and how C2CD3 regulates Wnt activity in the *ta²* during craniofacial skeletal development has not yet been described. Our future research will examine the impact loss of C2CD3-mediated ciliogenesis has on Wnt signaling.

BMP and FGF signaling pathways are also required for mandibular skeletogenesis (Ashe et al., 2012; Merrill et al., 2008; Mina et al., 2007), but there is a lack of understanding of how these signals are affected in ciliopathic backgrounds. The ciliopathic *Fuz*$^{-/-}$ mouse mutant exhibits craniofacial features that closely resemble FGF hyperactivation syndromes, such as craniosynostosis and high arched palate (Tabler et al., 2013). In addition, our previous studies with the *ta²* mutant have demonstrated that the developing MNP and maxillary prominence have increased FGF signaling (Schock et al., 2015). However, the mechanistic link between cilia and the FGF signaling pathway has not yet been established. In addition, it is unclear whether, and how, a BMP

Development (2021) 148, dev194175. doi:10.1242/dev.194175

signal is transduced through the primary cilium (reviewed by Kaku and Komatsu, 2017). Our future goals include gaining a broader understanding of how other signaling pathways essential for skeletal development are affected in ciliary mutants.

Pharmacological intervention could alleviate ciliopathic micrognathia

Bone is constantly remodeled through bone deposition and bone resorption. Disturbances in the skeletal environment caused by excessive bone remodeling lead to decreased jaw length and density (Ealba et al., 2015; Feng and McDonald, 2011). As bone remodeling requires both bone deposition and bone resorption, defects in either program can lead to bone remodeling diseases such as osteoporosis and osteopetrosis (Feng and McDonald, 2011). It has also been long established that osteoblasts and osteoclasts communicate to control bone remodeling through physical interaction and release of various growth factors and chemokines (Matsuo and Irie, 2008); however, how primary cilia mechanically or molecularly contribute to this communication has not yet been discovered. Previous studies have reported that primary cilia may play an antiresorptive role in osteocytes through increasing the RANKL/OPG ratio (Malone et al., 2007). Although our studies confirm this finding, as loss of cilia resulted in increased bone resorption in the *ta*^{2} mandible, future work on the molecular and mechanical control of bone resorption by primary cilia is necessary.

The discovery that bone remodeling contributes to ciliopathic micrognathia is a significant finding as it opens a potential avenue of therapeutic intervention. Studies have shown that bone resorption can be pharmacologically induced or depleted with recombinant forms of OPG and RANKL in avian models (Ealba et al., 2015). In addition, bisphosphonates have previously been used to decrease bone resorption by preventing osteoclast formation and inducing osteoclast apoptosis (Boonekamp et al., 1986; Löwik et al., 1988; Sato and Grasser, 1990). Lastly, specific αNAC polypeptides have the potential to induce osteoblastic maturation *in vivo* (Meury et al., 2010). Treating ciliopathic micrognathia models, including the *ta*^{2}, with these compounds during discrete temporal windows of remodeling is a focus of our ongoing research.

Mechano- and chemosensory mechanisms may also contribute to ciliopathic micrognathia

It is well-established that increased mechanical loading stimulates bone formation (reviewed by Robling and Turner, 2009), and numerous studies have demonstrated a role for primary cilia as mechanosensory organelles during skeletal development (Leucht et al., 2013; Malone et al., 2007; Temiyasathit and Jacobs, 2010; Temiyasathit et al., 2012). Conditional loss of cilia in osteoblasts and osteocytes causes reduced bone formation due to reduced loading (Temiyasathit et al., 2012), decreased osteogenic response during fracture healing (Leucht et al., 2013) and inhibition of fluid flow-induced expression of osteogenic markers (Malone et al., 2007). When cilia on murine osteoblasts were removed with chloral hydrate, there was a lack of mineral deposition as a response to oscillatory fluid flow, demonstrating the importance of cilia for bone development (Delaine-Smith et al., 2014).

Several studies have also suggested that a key role of the primary cilium is to function as a chemical sensor for extracellular Ca^{2+} (Delling et al., 2013; Nauli et al., 2016; Zayzafoon, 2006). Primary cilia possess membrane-based ion channels including PKD2L1 (TRPP3), which allow for intracellular flux of Ca^{2+} (DeCaen et al., 2013; Nauli et al., 2016). Although this theory is controversial (Delling et al., 2016), this is an interesting direction for future experimental work given that bone mineralization requires Ca^{2+}. Ca^{2+} is essential for bone mineralization as it precipitates with inorganic phosphate to form hydroxyapatite crystals in collagen-rich extracellular matrix (reviewed by Murshed, 2018). Low Ca^{2+} intake and incorporation lead to severe skeletogenic disorders, such as osteoporosis and osteopenia, which are presented with low osteoblast maturation and increased bone remodeling (Anderson, 1996; Dymling, 1964). Could C2CD3-mediated loss of cilia prevent Ca^{2+} processing or integration into skeletal elements? This question is particularly intriguing for the fact that bone deposition, differentiation and remodeling are connected to Ca^{2+} signaling (Delling et al., 2013; Nauli et al., 2016; Zayzafoon, 2006) and that C2CD3 contains several C2 Ca^{2+}-dependent domains that are very poorly understood. Future studies will help to address whether and how Ca^{2+} integration is affected in ciliopathic mutants, and will be crucial for the understanding of how micrognathia and other ciliopathic skeletal disorders can be treated.

MATERIALS AND METHODS

Avian embryo collection, genotyping and tissue preparation

Fertilized control and *ta*^{2} eggs were supplied from University of California, Davis, CA, USA. Embryos were incubated at 38.8°C for 5-13 days and then harvested for analysis. All embryos collected were staged according to the Hamburger-Hamilton staging system and genotyped as previously described (Chang et al., 2014; Hamburger and Hamilton, 1951). For all experiments, three control$^{+/+}$ and three *ta*^{2} embryos at each stage were used, unless noted otherwise in the text or figure descriptions. Embryos were fixed in 4% paraformaldehyde (PFA) overnight at 4°C, unless noted otherwise.

Whole-mount skeletal staining

Whole-mount skeletal staining was performed as previously described (Rigueur and Lyons, 2014) with several modifications. Briefly, embryos were collected in PBS and fixed in 95% ethanol (EtOH) overnight. To remove excess adipose tissue, embryos were incubated in acetone overnight. To stain cartilage, embryos were placed in 0.03% Alcian Blue solution (Sigma-Aldrich, A5268) for 2 h. Following cartilage staining, samples were washed with seven parts EtOH and three parts acetic acid until the solution was clear and incubated in 95% EtOH overnight. To stain bone, samples were incubated in 0.005% Alizarin Red S (Sigma-Aldrich, A5533) in 1% KOH for 3 h at room temperature and cleared in 1% KOH. Once cleared, samples were incubated in 50% glycerol/50% KOH solution. For imaging and long-term storage, samples were kept in 100% glycerol. Stained specimens were imaged using a Leica M165 FC stereo microscope system.

Skeletal element analysis

Mandibular and ceratobranchial length measurements were performed using Leica LAS X software. Alizarin Red-stained mandibles were measured from the distal tip of the dentary bone to the proximal edge of the surangular bone for each side of the mandible and then averaged. For the mandibular length and area measurements, Alizarin Red-stained mandibles were measured in mm or bones were traced in Fiji (Schindelin et al., 2012) and areas of each bone were measured and calculated in mm^{2}. Volumetric analysis of individual skeletal elements (voxel measurements) were taken from the µCT-analyzed embryos. Unpaired one-tailed Student's *t*-test was used for statistical analysis. $P<0.05$ was determined to be significant.

Micro-computed tomography

HH36 and HH39 mandibles were harvested, fixed in 4% PFA and stained with 0.005% Alizarin Red S in 1% KOH solution for 3 h at room temperature. The samples were further processed at the Preclinical Imaging Core in the University of Cincinnati Vontz Center for Molecular Studies, OH, USA. Mandibular surface and volume area were extracted from DICOM files and measured in voxels. These files were analyzed and processed in Imaris 9.3 (Bitplane, Oxford Instruments).

Development (2021) 148, dev194175. doi:10.1242/dev.194175

Histology

Hematoxylin and eosin (H&E) staining was performed using standard protocols. Pentachrome staining was performed as previously described with slight modifications, as methyl cellosolve acetate washes were substituted with xylene washes and slides were transferred to alkaline ethanol solution for 90 min (Olah et al., 1977). TRAP staining was performed on 8 µm thick frontal sections of undecalcified HH39 mandibles using the Acid Phosphatase Leukocyte (TRAP) kit (Sigma-Aldrich, 387A) following the manufacturer's protocol, with Fast Red Violet LB Solution (Sigma-Aldrich, 912) used in place of provided Fast Garnet GBC Solution.

Immunofluorescence

Whole mandible immunofluorescence was carried out as previously described with minor modifications (Williams et al., 2018). Femur and mandibles were sagittally and frontally sectioned at 8 µm. Triton-X concentration was increased to 1%, and the sections and embryos were incubated in blocking solution supplemented with 5% normal goat serum. Cleaved Caspase-3 (1:100, Cell Signaling Technology, 9661), Collagen Type I Alexa-Fluor 488 Conjugate (1:200, SouthernBiotech, 1310-30), Osteocalcin (1:20, Abcam, 17.0021) and Phospho-Histone H3 (1:200, Cell Signaling Technology, 9706) primary antibodies were used. The secondary antibodies used were goat anti-mouse-568 (1:250, Thermo Fisher Scientific, A-11004), goat anti-rabbit-647 (1:250, Thermo Fisher Scientific, A21244) and Sox9-Conjugate AlexaFluor-488 (1:100, Cell Signaling Technology, 94794). Nuclei counterstaining was carried out by incubation in 1 µg/ml DAPI in PBS+Triton 1% for 2 h and processed for clearing with Ce3D solution overnight (Li et al., 2017).

RNAscope *in situ* hybridization

HH29 heads, HH35 heads and HH39 mandibles were fixed in 4% PFA at 4°C for 16-24 h. HH35 heads and HH39 mandibles were decalcified in 19% EDTA solution at 4°C for 2 and 5 days, respectively. Samples were dehydrated in an ethanol series, washed in xylene, embedded in paraffin and sectioned at 8 µm thickness using a Sakura Accu-Cut SRM 200 microtome. Transcripts of *RUNX2* (ACD 571591), *HAND2* (ACD 571571-C2) and *DLX5* (ACD 571561) were detected using the RNAscope Multiplex Fluorescent V2 kit per the manufacturer's instructions. Transcripts of *SPP1* (ACD 571601), *ALPL* (ACD 837811) and *MMP13* (ACD 571581) were detected using RNAscope 2.5 HD Duplex Assay (ACD) per the manufacturer's instructions. Briefly, slides were baked in a hybridization oven for 1 h at 60°C, deparaffinized using xylene, dehydrated using 100% EtOH and allowed to dry completely at room temperature. Endogenous peroxidase activity was quenched using RNAscope Hydrogen Peroxide and washed using distilled water. Target retrieval was performed using 1× RNAscope Target Retrieval Buffer in an Oster steamer for 15 min, washed in distilled water, dehydrated in 100% EtOH and dried at 60°C. Slides were treated with ACD Protease Plus in an HybEZ II oven for 30 min at 40°C. Probes were hybridized for 2 h at 40°C in an HybEZ II oven. Amplification steps were performed as described by the manufacturer. Signal development for *RUNX2*, *HAND2* and *DLX5* were carried out using Cyanine 3 (PerkinElmer, NEL752001KT) diluted 1:500 in RNAscope Multiplex TSA Buffer. Signal amplification for *SPP1*, *ALPL* and *MMP13* was carried out using provided HRP-based Green chromogen. Slides were counterstained and mounted per the manufacturer's instructions and imaged using a Leica DM5000B upright microscope system.

Fluorescent *in situ* hybridization

Fluorescent whole mount *in situ* hybridization (FISH) was performed using digoxigenin-labeled riboprobes as previously described (Denkers et al., 2004). Antisense riboprobes against *DLX5* (NM_204159.1; primers F 5′-ATCAGGTCCTCCGACTTCCA-3′ and R 5′-ATACGACTCACTATAG-GGGATTTTCACCTGCG TCTGCG-3′), *HAND2* (NM_204966.2; primers F 5′-CGAGGAGAACCCCTACTTCC-3′ and R 5′-TAATACGACTCAC-TATAGGGCCTGTCCGCCCTTTGGTTT-3′) and *RUNX2* (NM_204128.1; primers F 5′-CGCATTCCTCATCCCAGTAT-3′ and R 5′-TAATACGACTC-ACTATAGGGTATGGAGTGCTGCTGGTCTG-3′) were designed to range from 600 to 800 bp. TSA Plus HRP-Fluorescence kits were used for both Cyanine 3 and Cyanine 5 fluorescence channels (PerkinElmer, NEL752001KT). For simultaneous SOX9 immunofluorescence, embryos were washed with Tris-NaCl-Tween (TNT) and incubated overnight in 5% normal goat serum in TNT. Nuclei were counterstained with DAPI. For the vector rendering, confocal images were loaded in Bitplane Imaris and the surface algorithm was run. The selection of the surface was made by subtracting the background and adjusting the brightness until no signal was detected outside of the surface. The spots rendering for PHH3 and CC3 were adjusted for the detection of 2 µm signals, and background subtraction was applied.

qRT-PCR

RNA was extracted using TRIzol reagent (Invitrogen) and cDNA was synthesized using SuperScript III (Invitrogen). HH39 mandibles were first frozen with liquid nitrogen and ground using a mortar and pestle to ensure homogenous extraction. SYBR Green Supermix (Bio-Rad) and a Quant6 Applied Biosytems qPCR machine were used to perform qRT-PCR. All the genes were normalized to GAPDH expression. Negative controls were performed by omitting the cDNA in the mixture. The level of expression for each gene was calculated using the $2^{-\Delta\Delta Cq}$ method (Livak and Schmittgen, 2001). Unpaired one-tailed Student's *t*-test was used for statistical analysis. $P<0.05$ was determined to be significant.

Acknowledgements

We thank Mary Delany and the University of California, Davis, Avian Facility, Jackie Pisenti and Kevin Bellido for maintenance and husbandry of the *talpid*^{2} colony. Technical assistance was given by Dr Matt Kofron and Evan Meyer for image acquisition and analysis (Confocal Imaging Core at Cincinnati Children's Hospital Medical Center) and Dr Lisa Lemen for µCT acquisition and analysis (Preclinical Imaging Core at the University of Cincinnati). We also thank members of the Brugmann lab for helpful comments and feedback, especially Dr Kelsey Elliott for her valuable help analyzing the RNA-seq data.

Competing interests

The authors declare no competing or financial interests.

Author contributions

Conceptualization: S.A.B.; Methodology: C.L.B.P.; Validation: C.L.B.P., E.C.B.; Formal analysis: S.A.B.; Investigation: C.L.B.P., E.C.B., M.A.-P.; Resources: S.A.B.; Writing - original draft: C.L.B.P., S.A.B.; Writing - review & editing: C.L.B.P., E.C.B., S.A.B.; Visualization: C.L.B.P., E.C.B., S.A.B.; Supervision: S.A.B.; Project administration: S.A.B.; Funding acquisition: S.A.B.

Funding

This study was funded by the National Institute of Dental and Craniofacial Research (R35 DE027557) and Shriners Hospitals for Children (543938) to S.A.B. Deposited in PMC for release after 12 months.

Supplementary information

Supplementary information available online at
https://dev.biologists.org/lookup/doi/10.1242/dev.194175.supplemental

Peer review history

The peer review history is available online at
https://dev.biologists.org/lookup/doi/10.1242/dev.194175.reviewer-comments.pdf

References

Abbott, Ü., Taylor, L. W. and Abplanalp, H. (1959). *A 2nd Talpid-like Mutation in the Fowl, Poultry Science*, pp. 1185-1185. Oxford Univ Press.

Abbott, Ü. K., Taylor, L. W. and Abplanalp, H. (1960). Studies with talpid2, an embryonic lethal of the fowl. *J. Hered.* **51**, 194-202. doi:10.1093/oxfordjournals.jhered.a106988

Abzhanov, A., Rodda, S. J., McMahon, A. P. and Tabin, C. J. (2007). Regulation of skeletogenic differentiation in cranial dermal bone. *Development* **134**, 3133-3144. doi:10.1242/dev.002709

Adel Al-Lami, H., Barrell, W. B. and Liu, K. J. (2016). Micrognathia in mouse models of ciliopathies. *Biochem. Soc. Trans.* **44**, 1753-1759. doi:10.1042/BST20160241

Anderson, J. J. B. (1996). Calcium, phosphorus and human bone development. *J. Nutr.* **126**, 1153S-1158S. doi:10.1093/jn/126.suppl_4.1153S

Arsov, T., Silva, D. G., O'Bryan, M. K., Sainsbury, A., Lee, N. J., Kennedy, C., Manji, S. S. M., Nelms, K., Liu, C., Vinuesa, C. G. et al. (2006). Fat aussie–a new Alström syndrome mouse showing a critical role for ALMS1 in obesity, diabetes, and spermatogenesis. *Mol. Endocrinol.* **20**, 1610-1622. doi:10.1210/me.2005-0494

Ashe, A., Butterfield, N. C., Town, L., Courtney, A. D., Cooper, A. N., Ferguson, C., Barry, R., Olsson, F., Liem, K. F., Jr, Parton, R. G. et al. (2012). Mutations in mouse Ift144 model the craniofacial, limb and rib defects in skeletal ciliopathies. *Hum. Mol. Genet.* **21**, 1808-1823. doi:10.1093/hmg/ddr613

Baker, K. and Beales, P. L. (2009). Making sense of cilia in disease: the human ciliopathies. *Am. J. Med. Genet. C Semin. Med. Genet.* **151C**, 281-295. doi:10.1002/ajmg.c.30231

Barr, A. R., Cooper, S., Heldt, F. S., Butera, F., Stoy, H., Mansfeld, J., Novák, B. and Bakal, C. (2017). DNA damage during S-phase mediates the proliferation-quiescence decision in the subsequent G1 via p21 expression. *Nat. Commun.* **8**, 14728. doi:10.1038/ncomms14728

Bartkova, J., Lukas, J., Strauss, M. and Bartek, J. (1998). Cyclin D3: requirement for G1/S transition and high abundance in quiescent tissues suggest a dual role in proliferation and differentiation. *Oncogene* **17**, 1027-1037. doi:10.1038/sj.onc.1202016

Behonick, D. J., Xing, Z., Lieu, S., Buckley, J. M., Lotz, J. C., Marcucio, R. S., Werb, Z., Miclau, T. and Colnot, C. (2007). Role of matrix metalloproteinase 13 in both endochondral and intramembranous ossification during skeletal regeneration. *PLoS ONE* **2**, e1150. doi:10.1371/journal.pone.0001150

Billmyre, K. K. and Klingensmith, J. (2015). Sonic hedgehog from pharyngeal arch 1 epithelium is necessary for early mandibular arch cell survival and later cartilage condensation differentiation. *Dev. Dyn.* **244**, 564-576. doi:10.1002/dvdy.24256

Boczek, N. J., Hopp, K., Benoit, L., Kraft, D., Cousin, M. A., Blackburn, P. R., Madsen, C. D., Oliver, G. R., Nair, A. A., Na, J. et al. (2018). Characterization of three ciliopathy pedigrees expands the phenotype associated with biallelic C2CD3 variants. *Eur. J. Hum. Genet.* **26**, 1797-1809. doi:10.1038/s41431-018-0222-3

Boonekamp, P. M., van der Wee-Pals, L. J., van Wijk-van Lennep, M. M., Thesing, C. W. and Bijvoet, O. L. (1986). Two modes of action of bisphosphonates on osteoclastic resorption of mineralized matrix. *Bone Miner.* **1**, 27-39. doi:10.1016/8756-3282(85)90012-2

Brugmann, S. A., Allen, N. C., James, A. W., Mekonnen, Z., Madan, E. and Helms, J. A. (2010). A primary cilia-dependent etiology for midline facial disorders. *Hum. Mol. Genet.* **19**, 1577-1592. doi:10.1093/hmg/ddq030

Cela, P., Hampl, M., Shylo, N. A., Christopher, K. J., Kavkova, M., Landova, M., Zikmund, T., Weatherbee, S. D., Kaiser, J. and Buchtova, M. (2018). Ciliopathy protein Tmem107 plays multiple roles in craniofacial development. *J. Dent. Res.* **97**, 108-117. doi:10.1177/0022034517732538

Chang, C.-F., Schock, E. N., O'Hare, E. A., Dodgson, J., Cheng, H. H., Muir, W. M., Edelmann, R. E., Delany, M. E. and Brugmann, S. A. (2014). The cellular and molecular etiology of the craniofacial defects in the avian ciliopathic mutant talpid2. *Development* **141**, 3003-3012. doi:10.1242/dev.105924

Chang, C.-F., Chang, Y.-T., Millington, G. and Brugmann, S. A. (2016a). Craniofacial ciliopathies reveal specific requirements for GLI proteins during development of the facial midline. *PLoS Genet.* **12**, e1006351. doi:10.1371/journal.pgen.1006351

Chang, Y.-T., Chaturvedi, P., Schock, E. N. and Brugmann, S. A. (2016b). Understanding mechanisms of GLI-mediated transcription during craniofacial development and disease using the ciliopathic mutant, talpid(2). *Front. Physiol.* **7**, 468. doi:10.3389/fphys.2016.00468

Choi, S. T., Kim, J. H., Kang, E.-J., Lee, S.-W., Park, M.-C., Park, Y.-B. and Lee, S.-K. (2008). Osteopontin might be involved in bone remodelling rather than in inflammation in ankylosing spondylitis. *Rheumatology (Oxf.)* **47**, 1775-1779. doi:10.1093/rheumatology/ken385

Collin, G. B., Cyr, E., Bronson, R., Marshall, J. D., Gifford, E. J., Hicks, W., Murray, S. A., Zheng, Q. Y., Smith, R. S., Nishina, P. M. et al. (2005). Alms1-disrupted mice recapitulate human Alström syndrome. *Hum. Mol. Genet.* **14**, 2323-2333. doi:10.1093/hmg/ddi235

Corbit, K. C., Shyer, A. E., Dowdle, W. E., Gaulden, J., Singla, V., Chen, M. H., Chuang, P. T. and Reiter, J. F. (2008). Kif3a constrains β-catenin-dependent Wnt signalling through dual ciliary and non-ciliary mechanisms. *Nat. Cell Biol.* **10**, 70-76. doi:10.1038/ncb1670

Cortés, C. R., McInerney-Leo, A. M., Vogel, I., Rondón Galeano, M. C., Leo, P. J., Harris, J. E., Anderson, L. K., Keith, P. A., Brown, M. A., Ramsing, M. et al. (2016). Mutations in human C2CD3 cause skeletal dysplasia and provide new insights into phenotypic and cellular consequences of altered C2CD3 function. *Sci. Rep.* **6**, 24083. doi:10.1038/srep24083

Couly, G., Grapin-Botton, A., Coltey, P. and Le Douarin, N. M. (1996). The regeneration of the cephalic neural crest, a problem revisited: the regenerating cells originate from the contralateral or from the anterior and posterior neural fold. *Development* **122**, 3393-3407.

Cui, N., Hu, M. and Khalil, R. A. (2017). Biochemical and biological attributes of matrix metalloproteinases. *Prog. Mol. Biol. Transl. Sci.* **147**, 1-73. doi:10.1016/bs.pmbts.2017.02.005

Davenport, J. R., Watts, A. J., Roper, V. C., Croyle, M. J., van Groen, T., Wyss, J. M., Nagy, T. R., Kesterson, R. A. and Yoder, B. K. (2007). Disruption of intraflagellar transport in adult mice leads to obesity and slow-onset cystic kidney disease. *Curr. Biol.* **17**, 1586-1594. doi:10.1016/j.cub.2007.08.034

DeCaen, P. G., Delling, M., Vien, T. N. and Clapham, D. E. (2013). Direct recording and molecular identification of the calcium channel of primary cilia. *Nature* **504**, 315-318. doi:10.1038/nature12832

Delaine-Smith, R. M., Sittichokechaiwut, A. and Reilly, G. C. (2014). Primary cilia respond to fluid shear stress and mediate flow-induced calcium deposition in osteoblasts. *FASEB J.* **28**, 430-439. doi:10.1096/fj.13-231894

Delling, M., DeCaen, P. G., Doerner, J. F., Febvay, S. and Clapham, D. E. (2013). Primary cilia are specialized calcium signalling organelles. *Nature* **504**, 311-314. doi:10.1038/nature12833

Delling, M., Indzhykulian, A. A., Liu, X., Li, Y., Xie, T., Corey, D. P. and Clapham, D. E. (2016). Primary cilia are not calcium-responsive mechanosensors. *Nature* **531**, 656-660. doi:10.1038/nature17426

Denkers, N., García-Villalba, P., Rodesch, C. K., Nielson, K. R. and Mauch, T. J. (2004). FISHing for chick genes: Triple-label whole-mount fluorescence in situ hybridization detects simultaneous and overlapping gene expression in avian embryos. *Dev. Dyn.* **229**, 651-657. doi:10.1002/dvdy.20005

Dixon, J., Jones, N. C., Sandell, L. L., Jayasinghe, S. M., Crane, J., Rey, J.-P., Dixon, M. J. and Trainor, P. A. (2006). Tcof1/Treacle is required for neural crest cell formation and proliferation deficiencies that cause craniofacial abnormalities. *Proc. Natl. Acad. Sci. USA* **103**, 13403-13408. doi:10.1073/pnas.0603730103

Doxsey, S., Zimmerman, W. and Mikule, K. (2005). Centrosome control of the cell cycle. *Trends Cell Biol.* **15**, 303-311. doi:10.1016/j.tcb.2005.04.008

Dvorak, L. and Fallon, J. F. (1992). The talpid2 chick limb has weak polarizing activity and can respond to retinoic acid and polarizing zone signal. *Dev. Dyn.* **193**, 40-48. doi:10.1002/aja.1001930107

Dymling, J. F. (1964). Calcium kinetics in osteopenia and parathyroid disease. *Acta Med. Scand.* **175** suppl. 408, 401-456.

Ealba, E. L., Jheon, A. H., Hall, J., Curantz, C., Butcher, K. D. and Schneider, R. A. (2015). Neural crest-mediated bone resorption is a determinant of species-specific jaw length. *Dev. Biol.* **408**, 151-163. doi:10.1016/j.ydbio.2015.10.001

Ede, D. A. and Kelly, W. A. (1964a). Developmental abnormalities in the head region of the talpid mutant of the fowl. *J. Embryol. Exp. Morphol.* **12**, 161-182.

Ede, D. A. and Kelly, W. A. (1964b). Developmental abnormalities in the trunk and limbs of the Talpid3 mutant of the fowl. *J. Embryol. Exp. Morphol.* **12**, 339-356.

Ek-Rylander, B., Flores, M., Wendel, M., Heinegard, D. and Andersson, G. (1994). Dephosphorylation of osteopontin and bone sialoprotein by osteoclastic tartrate-resistant acid phosphatase. Modulation of osteoclast adhesion in vitro. *J. Biol. Chem.* **269**, 14853-14856. doi:10.1016/s0021-9258(17)36541-9

el-Deiry, W. S., Tokino, T., Velculescu, V. E., Levy, D. B., Parsons, R., Trent, J. M., Lin, D., Mercer, W. E., Kinzler, K. W. and Vogelstein, B. (1993). WAF1, a potential mediator of p53 tumor suppression. *Cell* **75**, 817-825. doi:10.1016/0092-8674(93)90500-P

Elliott, K. H., Chen, X., Salomone, J., Chaturvedi, P., Schultz, P. A., Balchand, S. K., Servetas, J. D., Zuniga, A., Zeller, R., Gebelein, B. et al. (2020). Gli3 utilizes Hand2 to synergistically regulate tissue-specific transcriptional networks. *eLife* **9**, e56450. doi:10.7554/eLife.56450

Engsig, M. T., Chen, Q.-J., Vu, T. H., Pedersen, A.-C., Therkidsen, B., Lund, L. R., Henriksen, K., Lenhard, T., Foged, N. T., Werb, Z. et al. (2000). Matrix metalloproteinase 9 and vascular endothelial growth factor are essential for osteoclast recruitment into developing long bones. *J. Cell Biol.* **151**, 879-890. doi:10.1083/jcb.151.4.879

Feng, X. and McDonald, J. M. (2011). Disorders of bone remodeling. *Annu. Rev. Pathol.* **6**, 121-145. doi:10.1146/annurev-pathol-011110-130203

Franz-Odendaal, T. A. (2011). Induction and patterning of intramembranous bone. *Front. Biosci.* **16**, 2734-2746. doi:10.2741/3882

Funato, N., Chapman, S. L., McKee, M. D., Funato, H., Morris, J. A., Shelton, J. M., Richardson, J. A. and Yanagisawa, H. (2009). Hand2 controls osteoblast differentiation in the branchial arch by inhibiting DNA binding of Runx2. *Development* **136**, 615-625. doi:10.1242/dev.029355

Goetz, S. C. and Anderson, K. V. (2010). The primary cilium: a signalling centre during vertebrate development. *Nat. Rev. Genet.* **11**, 331-344. doi:10.1038/nrg2774

Gray, R. S., Abitua, P. B., Wlodarczyk, B. J., Szabo-Rogers, H. L., Blanchard, O., Lee, I., Weiss, G. S., Liu, K. J., Marcotte, E. M., Wallingford, J. B. et al. (2009). The planar cell polarity effector Fuz is essential for targeted membrane trafficking, ciliogenesis and mouse embryonic development. *Nat. Cell Biol.* **11**, 1225-1232. doi:10.1038/ncb1966

Guntur, A. R., Le, P. T., Farber, C. R. and Rosen, C. J. (2014). Bioenergetics during calvarial osteoblast differentiation reflect strain differences in bone mass. *Endocrinology* **155**, 1589-1595. doi:10.1210/en.2013-1974

Hall, J., Jheon, A. H., Ealba, E. L., Eames, B. F., Butcher, K. D., Mak, S.-S., Ladher, R., Alliston, T. and Schneider, R. A. (2014). Evolution of a developmental mechanism: species-specific regulation of the cell cycle and the timing of events during craniofacial osteogenesis. *Dev. Biol.* **385**, 380-395. doi:10.1016/j.ydbio.2013.11.011

Hamburger, V. and Hamilton, H. L. (1951). A series of normal stages in the development of the chick embryo. *J. Morphol.* **88**, 49-92. doi:10.1002/jmor.1050880104

Harris, M. P., Hasso, S. M., Ferguson, M. W. J. and Fallon, J. F. (2006). The development of archosaurian first-generation teeth in a chicken mutant. *Curr. Biol.* **16**, 371-377. doi:10.1016/j.cub.2005.12.047

Haycraft, C. J., Banizs, B., Aydin-Son, Y., Zhang, Q., Michaud, E. J. and Yoder, B. K. (2005). Gli2 and Gli3 localize to cilia and require the intraflagellar transport protein polaris for processing and function. *PLoS Genet.* **1**, e53. doi:10.1371/journal.pgen.0010053

Holleville, N., Matéos, S., Bontoux, M., Bollerot, K. and Monsoro-Burq, A. H. (2007). Dlx5 drives Runx2 expression and osteogenic differentiation in developing cranial suture mesenchyme. *Dev. Biol.* **304**, 860-874. doi:10.1016/j.ydbio.2007.01.003

Hoover, A. N., Wynkoop, A., Zeng, H., Jia, J., Niswander, L. A. and Liu, A. (2008). C2cd3 is required for cilia formation and Hedgehog signaling in mouse. *Development* **135**, 4049-4058. doi:10.1242/dev.029835

Huang, P. and Schier, A. F. (2009). Dampened Hedgehog signaling but normal Wnt signaling in zebrafish without cilia. *Development* **136**, 3089-3098. doi:10.1242/dev.041343

Huangfu, D. and Anderson, K. V. (2005). Cilia and Hedgehog responsiveness in the mouse. *Proc. Natl. Acad. Sci. USA* **102**, 11325-11330. doi:10.1073/pnas.0505328102

Huangfu, D., Liu, A., Rakeman, A. S., Murcia, N. S., Niswander, L. and Anderson, K. V. (2003). Hedgehog signalling in the mouse requires intraflagellar transport proteins. *Nature* **426**, 83-87. doi:10.1038/nature02061

Ilizarov, G. A. (1988). The principles of the Ilizarov method. *Bull. Hosp. Jt Dis. Orthop. Inst.* **48**, 1-11.

Izawa, I., Goto, H., Kasahara, K. and Inagaki, M. (2015). Current topics of functional links between primary cilia and cell cycle. *Cilia* **4**, 12. doi:10.1186/s13630-015-0021-1

Jeong, J., Mao, J., Tenzen, T., Kottmann, A. H. and McMahon, A. P. (2004). Hedgehog signaling in the neural crest cells regulates the patterning and growth of facial primordia. *Genes Dev.* **18**, 937-951. doi:10.1101/gad.1190304

Jiang, Z., Von den Hoff, J. W., Torensma, R., Meng, L. and Bian, Z. (2014). Wnt16 is involved in intramembranous ossification and suppresses osteoblast differentiation through the Wnt/β-catenin pathway. *J. Cell. Physiol.* **229**, 384-392. doi:10.1002/jcp.24460

Johansson, N., Saarialho-Kere, U., Airola, K., Herva, R., Nissinen, L., Westermarck, J., Vuorio, E., Heino, J. and Kähäri, V.-M. (1997). Collagenase-3 (MMP-13) is expressed by hypertrophic chondrocytes, periosteal cells, and osteoblasts during human fetal bone development. *Dev. Dyn.* **208**, 387-397. doi:10.1002/(SICI)1097-0177(199703)208:3<387::AID-AJA9>3.0.CO;2-E

Jones, N. C., Lynn, M. L., Gaudenz, K., Sakai, D., Aoto, K., Rey, J.-P., Glynn, E. F., Ellington, L., Du, C., Dixon, J. et al. (2008). Prevention of the neurocristopathy Treacher Collins syndrome through inhibition of p53 function. *Nat. Med.* **14**, 125-133. doi:10.1038/nm1725

Kaku, M. and Komatsu, Y. (2017). Functional diversity of ciliary proteins in bone development and disease. *Curr. Osteoporos Rep.* **15**, 96-102. doi:10.1007/s11914-017-0351-6

Kawasaki, M., Izu, Y., Hayata, T., Ideno, H., Nifuji, A., Sheffield, V. C., Ezura, Y. and Noda, M. (2017). Bardet-Biedl syndrome 3 regulates the development of cranial base midline structures. *Bone* **101**, 179-190. doi:10.1016/j.bone.2016.02.017

Kim, S. and Tsiokas, L. (2011). Cilia and cell cycle re-entry: more than a coincidence. *Cell Cycle* **10**, 2683-2690. doi:10.4161/cc.10.16.17009

Kim, S., Lee, K., Choi, J.-H., Ringstad, N. and Dynlacht, B. D. (2015). Nek2 activation of Kif24 ensures cilium disassembly during the cell cycle. *Nat. Commun.* **6**, 8087. doi:10.1038/ncomms9087

Kim, M., Suh, Y.-A., Oh, J.-H., Lee, B. R., Kim, J. and Jang, S. J. (2016). KIF3A binds to β-arrestin for suppressing Wnt/β-catenin signalling independently of primary cilia in lung cancer. *Sci. Rep.* **6**, 32770. doi:10.1038/srep32770

Kitamura, A., Kawasaki, M., Kawasaki, K., Meguro, F., Yamada, A., Nagai, T., Kodama, Y., Trakanant, S., Sharpe, P. T., Maeda, T. et al. (2020). Ift88 is involved in mandibular development. *J. Anat.* **236**, 317-324. doi:10.1111/joa.13096

Kobayashi, T. and Dynlacht, B. D. (2011). Regulating the transition from centriole to basal body. *J. Cell Biol.* **193**, 435-444. doi:10.1083/jcb.201101005

Kobayashi, H., Gao, Y., Ueta, C., Yamaguchi, A. and Komori, T. (2000). Multilineage differentiation of Cbfa1-deficient calvarial cells in vitro. *Biochem. Biophys. Res. Commun.* **273**, 630-636. doi:10.1006/bbrc.2000.2981

Kolpakova-Hart, E., Jinnin, M., Hou, B., Fukai, N. and Olsen, B. R. (2007). Kinesin-2 controls development and patterning of the vertebrate skeleton by Hedgehog- and Gli3-dependent mechanisms. *Dev. Biol.* **309**, 273-284. doi:10.1016/j.ydbio.2007.07.018

Komori, T., Yagi, H., Nomura, S., Yamaguchi, A., Sasaki, K., Deguchi, K., Shimizu, Y., Bronson, R. T., Gao, Y.-H., Inada, M. et al. (1997). Targeted disruption of Cbfa1 results in a complete lack of bone formation owing to maturational arrest of osteoblasts. *Cell* **89**, 755-764. doi:10.1016/S0092-8674(00)80258-5

Kontges, G. and Lumsden, A. (1996). Rhombencephalic neural crest segmentation is preserved throughout craniofacial ontogeny. *Development* **122**, 3229-3242.

Lancaster, M. A., Schroth, J. and Gleeson, J. G. (2011). Subcellular spatial regulation of canonical Wnt signalling at the primary cilium. *Nat. Cell Biol.* **13**, 700-707. doi:10.1038/ncb2259

Le Douarin, N. (1982). *The Neural Crest*. Cambridge: Cambridge University Press.

Lee, M.-H., Kim, Y.-J., Kim, H.-J., Park, H.-D., Kang, A.-R., Kyung, H.-M., Sung, J.-H., Wozney, J. M., Kim, H.-J. and Ryoo, H.-M. (2003). BMP-2-induced Runx2 expression is mediated by Dlx5, and TGF-β1 opposes the BMP-2-induced osteoblast differentiation by suppression of Dlx5 expression. *J. Biol. Chem.* **278**, 34387-34394. doi:10.1074/jbc.M211386200

Lenton, K., James, A. W., Manu, A., Brugmann, S. A., Birker, D., Nelson, E. R., Leucht, P., Helms, J. A. and Longaker, M. T. (2011). Indian hedgehog positively regulates calvarial ossification and modulates bone morphogenetic protein signaling. *Genesis* **49**, 784-796. doi:10.1002/dvg.20768

Leucht, P., Monica, S. D., Temiyasathit, S., Lenton, K., Manu, A., Longaker, M. T., Jacobs, C. R., Spilker, R. L., Guo, H., Brunski, J. B. et al. (2013). Primary cilia act as mechanosensors during bone healing around an implant. *Med. Eng. Phys.* **35**, 392-402. doi:10.1016/j.medengphy.2012.06.005

Li, W. Z., Germain, R. N. and Gerner, M. Y. (2017). Multiplex, quantitative cellular analysis in large tissue volumes with clearing-enhanced 3D microscopy (C(e)3D). *Proc. Natl. Acad. Sci. USA* **114**, E7321-E7330. doi:10.1073/pnas.1708981114

Lillie, F. R. and Hamilton, H. L. (1952). *Lillie's Development of the Chick: An Introduction to Embryology*, 3rd edn. New York: Holt.

Liu, A., Wang, B. and Niswander, L. A. (2005). Mouse intraflagellar transport proteins regulate both the activator and repressor functions of Gli transcription factors. *Development* **132**, 3103-3111. doi:10.1242/dev.01894

Livak, K. J. and Schmittgen, T. D. (2001). Analysis of relative gene expression data using real-time quantitative PCR and the $2^{-\Delta\Delta CT}$ method. *Methods* **25**, 402-408. doi:10.1006/meth.2001.1262

Lorberbaum, D. S., Ramos, A. I., Peterson, K. A., Carpenter, B. S., Parker, D. S., De, S., Hillers, L. E., Blake, V. M., Nishi, Y., McFarlane, M. R. et al. (2016). An ancient yet flexible cis-regulatory architecture allows localized Hedgehog tuning by patched/Ptch1. *eLife* **5**, e13550. doi:10.7554/eLife.13550

Löwik, C. W. G. M., van der Pluijm, G., van der Wee-Pals, L. J. A., van Treslong-De Groot, H. B. and Bijvoet, O. L. M. (1988). Migration and phenotypic transformation of osteoclast precursors into mature osteoclasts: the effect of a bisphosphonate. *J. Bone Miner. Res.* **3**, 185-192. doi:10.1002/jbmr.5650030210

Malone, A. M. D., Anderson, C. T., Tummala, P., Kwon, R. Y., Johnston, T. R., Stearns, T. and Jacobs, C. R. (2007). Primary cilia mediate mechanosensing in bone cells by a calcium-independent mechanism. *Proc. Natl. Acad. Sci. USA* **104**, 13325-13330. doi:10.1073/pnas.0700636104

Marion, V., Stoetzel, C., Schlicht, D., Messaddeq, N., Koch, M., Flori, E., Danse, J. M., Mandel, J.-L. and Dollfus, H. (2009). Transient ciliogenesis involving Bardet-Biedl syndrome proteins is a fundamental characteristic of adipogenic differentiation. *Proc. Natl. Acad. Sci. USA* **106**, 1820-1825. doi:10.1073/pnas.0812518106

Matsuo, K. and Irie, N. (2008). Osteoclast-osteoblast communication. *Arch. Biochem. Biophys.* **473**, 201-209. doi:10.1016/j.abb.2008.03.027

Merrill, A. E., Eames, B. F., Weston, S. J., Heath, T. and Schneider, R. A. (2008). Mesenchyme-dependent BMP signaling directs the timing of mandibular osteogenesis. *Development* **135**, 1223-1234. doi:10.1242/dev.015933

Meury, T., Akhouayri, O., Jafarov, T., Mandic, V. and St-Arnaud, R. (2010). Nuclear αNAC influences bone matrix mineralization and osteoblast maturation in vivo. *Mol. Cell. Biol.* **30**, 43-53. doi:10.1128/MCB.00378-09

Millington, G., Elliott, K. H., Chang, Y.-T., Chang, C.-F., Dlugosz, A. and Brugmann, S. A. (2017). Cilia-dependent GLI processing in neural crest cells is required for tongue development. *Dev. Biol.* **424**, 124-137. doi:10.1016/j.ydbio.2017.02.021

Mina, M., Havens, B. and Velonis, D. A. (2007). FGF signaling in mandibular skeletogenesis. *Orthod. Craniofac. Res.* **10**, 59-66. doi:10.1111/j.1601-6343.2007.00385.x

Minkin, C. (1982). Bone acid phosphatase: tartrate-resistant acid phosphatase as a marker of osteoclast function. *Calcif. Tissue Int.* **34**, 285-290. doi:10.1007/BF02411252

Morgan, D., Eley, L., Sayer, J., Strachan, T., Yates, L. M., Craighead, A. S. and Goodship, J. A. (2002). Expression analyses and interaction with the anaphase promoting complex protein Apc2 suggest a role for inversin in primary cilia and involvement in the cell cycle. *Hum. Mol. Genet.* **11**, 3345-3350. doi:10.1093/hmg/11.26.3345

Mori-Akiyama, Y., Akiyama, H., Rowitch, D. H. and de Crombrugghe, B. (2003). Sox9 is required for determination of the chondrogenic cell lineage in the cranial neural crest. *Proc. Natl. Acad. Sci. USA* **100**, 9360-9365. doi:10.1073/pnas.1631288100

Muñoz-Sanjuán, I., Cooper, M. K., Beachy, P. A., Fallon, J. F. and Nathans, J. (2001). Expression and regulation of chicken fibroblast growth factor homologous factor (FHF)-4 during craniofacial morphogenesis. *Dev. Dyn.* **220**, 238-245.<238::AID-DVDY1104>3.0.CO;2-T

Murshed, M. (2018). Mechanism of bone mineralization. *Cold Spring Harb. Perspect. Med.* **8**, a031229. doi:10.1101/cshperspect.a031229

Nauli, S. M., Pala, R. and Kleene, S. J. (2016). Calcium channels in primary cilia. *Curr. Opin Nephrol. Hypertens.* **25**, 452-458. doi:10.1097/MNH.0000000000000251

Ng, L.-J., Wheatley, S., Muscat, G. E. O., Conway-Campbell, J., Bowles, J., Wright, E., Bell, D. M., Tam, P. P. L., Cheah, K. S. E. and Koopman, P. (1997). SOX9 binds DNA, activates transcription, and coexpresses with type II collagen during chondrogenesis in the mouse. *Dev. Biol.* **183**, 108-121. doi:10.1006/dbio.1996.8487

Nigg, E. A. and Stearns, T. (2011). The centrosome cycle: centriole biogenesis, duplication and inherent asymmetries. *Nat. Cell Biol.* **13**, 1154-1160. doi:10.1038/ncb2345

Ocbina, P. J. R., Tuson, M. and Anderson, K. V. (2009). Primary cilia are not required for normal canonical Wnt signaling in the mouse embryo. *PLoS ONE* **4**, e6839. doi:10.1371/journal.pone.0006839

Olah, A. J., Simon, A., Gaudy, M., Herrmann, W. and Schenk, R. K. (1977). Differential staining of calcified tissues in plastic embedded microtome sections by a modification of Movat's pentachrome stain. *Stain Technol.* **52**, 331-337. doi:10.3109/10520297709116809

Otto, F., Thornell, A. P., Crompton, T., Denzel, A., Gilmour, K. C., Rosewell, I. R., Stamp, G. W. H., Beddington, R. S. P., Mundlos, S., Olsen, B. R. et al. (1997). Cbfa1, a candidate gene for cleidocranial dysplasia syndrome, is essential for osteoblast differentiation and bone development. *Cell* **89**, 765-771. doi:10.1016/S0092-8674(00)80259-7

Pampliega, O., Orhon, I., Patel, B., Sridhar, S., Díaz-Carretero, A., Beau, I., Codogno, P., Satir, B. H., Satir, P. and Cuervo, A. M. (2013). Functional interaction between autophagy and ciliogenesis. *Nature* **502**, 194-200. doi:10.1038/nature12639

Pinero, G. J., Farach-Carson, M. C., Devoll, R. E., Aubin, J. E., Brunn, J. C. and Butler, W. T. (1995). Bone matrix proteins in osteogenesis and remodelling in the neonatal rat mandible as studied by immunolocalization of osteopontin, bone sialoprotein, α2HS-glycoprotein and alkaline phosphatase. *Arch. Oral Biol.* **40**, 145-155. doi:10.1016/0003-9969(94)00144-Z

Pugacheva, E. N., Jablonski, S. A., Hartman, T. R., Henske, E. P. and Golemis, E. A. (2007). HEF1-dependent Aurora A activation induces disassembly of the primary cilium. *Cell* **129**, 1351-1363. doi:10.1016/j.cell.2007.04.035

Qi, Y., Li, X., Chang, C., Xu, F., He, Q., Zhao, Y. and Wu, L. (2017). Ribosomal protein L23 negatively regulates cellular apoptosis via the RPL23/Miz-1/c-Myc circuit in higher-risk myelodysplastic syndrome. *Sci. Rep.* **7**, 2323. doi:10.1038/s41598-017-02403-x

Qing, H., Ardeshirpour, L., Pajevic, P. D., Dusevich, V., Jähn, K., Kato, S., Wysolmerski, J. and Bonewald, L. F. (2012). Demonstration of osteocytic perilacunar/canalicular remodeling in mice during lactation. *J. Bone Miner. Res.* **27**, 1018-1029. doi:10.1002/jbmr.1567

Regan, J. N., Lim, J., Shi, Y., Joeng, K. S., Arbeit, J. M., Shohet, R. V. and Long, F. (2014). Up-regulation of glycolytic metabolism is required for HIF1α-driven bone formation. *Proc. Natl. Acad. Sci. USA* **111**, 8673-8678. doi:10.1073/pnas.1324290111

Reponen, P., Sahlberg, C., Munaut, C., Thesleff, I. and Tryggvason, K. (1994). High expression of 92-kD type IV collagenase (gelatinase B) in the osteoclast lineage during mouse development. *J. Cell Biol.* **124**, 1091-1102. doi:10.1083/jcb.124.6.1091

Rigueur, D. and Lyons, K. M. (2014). Whole-mount skeletal staining. *Methods Mol. Biol.* **1130**, 113-121. doi:10.1007/978-1-62703-989-5_9

Robert, A., Margall-Ducos, G., Guidotti, J.-E., Bregerie, O., Celati, C., Brechot, C. and Desdouets, C. (2007). The intraflagellar transport component IFT88/polaris is a centrosomal protein regulating G1-S transition in non-ciliated cells. *J. Cell Sci.* **120**, 628-637. doi:10.1242/jcs.03366

Robling, A. G. and Turner, C. H. (2009). Mechanical signaling for bone modeling and remodeling. *Crit. Rev. Eukaryot. Gene Expr.* **19**, 319-338. doi:10.1615/CritRevEukarGeneExpr.v19.i4.50

Rodrigues, A. M., Caetano-Lopes, J., Vale, A. C., Vidal, B., Lopes, A., Aleixo, I., Polido-Pereira, J., Sepriano, A., Perpétuo, I. P., Monteiro, J. et al. (2012). Low osteocalcin/collagen type I bone gene expression ratio is associated with hip fragility fractures. *Bone* **51**, 981-989. doi:10.1016/j.bone.2012.08.129

Ross, A. J., May-Simera, H., Eichers, E. R., Kai, M., Hill, J., Jagger, D. J., Leitch, C. C., Chapple, J. P., Munro, P. M., Fisher, S. et al. (2005). Disruption of Bardet-Biedl syndrome ciliary proteins perturbs planar cell polarity in vertebrates. *Nat. Genet.* **37**, 1135-1140. doi:10.1038/ng1644

Rutkovskiy, A., Stensløkken, K.-O. and Vaage, I. J. (2016). Osteoblast differentiation at a glance. *Med. Sci. Monit. Basic Res.* **22**, 95-106. doi:10.12659/MSMBR.901142

Sato, M. and Grasser, W. (1990). Effects of bisphosphonates on isolated rat osteoclasts as examined by reflected light microscopy. *J. Bone Miner. Res.* **5**, 31-40. doi:10.1002/jbmr.5650050107

Schindelin, J., Arganda-Carreras, I., Frise, E., Kaynig, V., Longair, M., Pietzsch, T., Preibisch, S., Rueden, C., Saalfeld, S., Schmid, B. et al. (2012). Fiji: an open-source platform for biological-image analysis. *Nat. Methods* **9**, 676-682. doi:10.1038/nmeth.2019

Schneider, R. A., Hu, D. and Helms, J. A. (1999). From head to toe: conservation of molecular signals regulating limb and craniofacial morphogenesis. *Cell Tissue Res.* **296**, 103-109. doi:10.1007/s004410051271

Schock, E. N. and Brugmann, S. A. (2017). Discovery, diagnosis, and etiology of craniofacial ciliopathies. *Cold Spring Harb. Perspect. Biol.* **9**, a028258. doi:10.1101/cshperspect.a028258

Schock, E. N., Chang, C.-F., Struve, J. N., Chang, Y.-T., Chang, J., Delany, M. E. and Brugmann, S. A. (2015). Using the avian mutant talpid2 as a disease model for understanding the oral-facial phenotypes of oral-facial-digital syndrome. *Dis. Model. Mech.* **8**, 855-866. doi:10.1242/dmm.020222

Schock, E. N., Chang, C.-F., Youngworth, I. A., Davey, M. G., Delany, M. E. and Brugmann, S. A. (2016). Utilizing the chicken as an animal model for human craniofacial ciliopathies. *Dev. Biol.* **415**, 326-337. doi:10.1016/j.ydbio.2015.10.024

Shimoyama, A., Wada, M., Ikeda, F., Hata, K., Matsubara, T., Nifuji, A., Noda, M., Amano, K., Yamaguchi, A., Nishimura, R. et al. (2007). Ihh/Gli2 signaling promotes osteoblast differentiation by regulating Runx2 expression and function. *Mol. Biol. Cell* **18**, 2411-2418. doi:10.1091/mbc.e06-08-0743

Simons, M., Gloy, J., Ganner, A., Bullerkotte, A., Bashkurov, M., Krönig, C., Schermer, B., Benzing, T., Cabello, O. A., Jenny, A. et al. (2005). Inversin, the gene product mutated in nephronophthisis type II, functions as a molecular switch between Wnt signaling pathways. *Nat. Genet.* **37**, 537-543. doi:10.1038/ng1552

Tabler, J. M., Barrell, W. B., Szabo-Rogers, H. L., Healy, C., Yeung, Y., Perdiguero, E. G., Schulz, C., Yannakoudakis, B. Z., Mesbahi, A., Wlodarczyk, B. et al. (2013). Fuz mutant mice reveal shared mechanisms between ciliopathies and FGF-related syndromes. *Dev. Cell* **25**, 623-635. doi:10.1016/j.devcel.2013.05.021

Tang, S. Y., Herber, R. P., Ho, S. P. and Alliston, T. (2012). Matrix metalloproteinase-13 is required for osteocytic perilacunar remodeling and maintains bone fracture resistance. *J. Bone Miner. Res.* **27**, 1936-1950. doi:10.1002/jbmr.1646

Tang, Z., Lin, M. G., Stowe, T. R., Chen, S., Zhu, M., Stearns, T., Franco, B. and Zhong, Q. (2013). Autophagy promotes primary ciliogenesis by removing OFD1 from centriolar satellites. *Nature* **502**, 254-257. doi:10.1038/nature12606

Temiyasathit, S. and Jacobs, C. R. (2010). Osteocyte primary cilium and its role in bone mechanotransduction. *Ann. N. Y. Acad. Sci.* **1192**, 422-428. doi:10.1111/j.1749-6632.2009.05243.x

Temiyasathit, S., Tang, W. J., Leucht, P., Anderson, C. T., Monica, S. D., Castillo, A. B., Helms, J. A., Stearns, T. and Jacobs, C. R. (2012). Mechanosensing by the primary cilium: deletion of Kif3A reduces bone formation due to loading. *PLoS ONE* **7**, e33368. doi:10.1371/journal.pone.0033368

Thauvin-Robinet, C., Lee, J. S., Lopez, E., Herranz-Perez, V., Shida, T., Franco, B., Jego, L., Ye, F., Pasquier, L., Loget, P. et al. (2014). The oral-facial-digital syndrome gene C2CD3 encodes a positive regulator of centriole elongation. *Nat. Genet.* **46**, 905-911. doi:10.1038/ng.3031

Tian, H., Feng, J., Li, J., Ho, T.-V., Yuan, Y., Liu, Y., Brindopke, F., Figueiredo, J. C., Magee, W., III, Sanchez-Lara, P. A. et al. (2017). Intraflagellar transport 88 (IFT88) is crucial for craniofacial development in mice and is a candidate gene for human cleft lip and palate. *Hum. Mol. Genet.* **26**, 860-872. doi:10.1093/hmg/ddx002

Tucker, R. W., Pardee, A. B. and Fujiwara, K. (1979). Centriole ciliation is related to quiescence and DNA synthesis in 3T3 cells. *Cell* **17**, 527-535. doi:10.1016/0092-8674(79)90261-7

Wang, F., Flanagan, J., Su, N., Wang, L. C., Bui, S., Nielson, A., Wu, X., Vo, H. T., Ma, X. J. and Luo, Y. (2012). RNAscope: a novel in situ RNA analysis platform for formalin-fixed, paraffin-embedded tissues. *J. Mol. Diagn.* **14**, 22-29. doi:10.1016/j.jmoldx.2011.08.002

Watanabe, M., Kawasaki, M., Kawasaki, K., Kitamura, A., Nagai, T., Kodama, Y., Meguro, F., Yamada, A., Sharpe, P. T., Maeda, T. et al. (2019). Ift88 limits bone formation in maxillary process through suppressing apoptosis. *Arch. Oral Biol.* **101**, 43-50. doi:10.1016/j.archoralbio.2019.02.017

Williams, R. M., Senanayake, U., Artibani, M., Taylor, G., Wells, D., Ahmed, A. A. and Sauka-Spengler, T. (2018). Genome and epigenome engineering CRISPR toolkit for in vivo modulation of cis-regulatory interactions and gene expression in the chicken embryo. *Development* **145**, dev160333. doi:10.1242/dev.160333

Xu, J., Liu, H., Lan, Y., Adam, M., Clouthier, D. E., Potter, S. and Jiang, R. (2019). Hedgehog signaling patterns the oral-aboral axis of the mandibular arch. *eLife* **8**, e40315. doi:10.7554/eLife.40315

Ye, X., Zeng, H., Ning, G., Reiter, J. F. and Liu, A. (2014). C2cd3 is critical for centriolar distal appendage assembly and ciliary vesicle docking in mammals. *Proc. Natl. Acad. Sci. USA* **111**, 2164-2169. doi:10.1073/pnas.1318737111

Yeh, C., Li, A., Chuang, J. Z., Saito, M., Cáceres, A. and Sung, C. H. (2013). IGF-1 activates a cilium-localized noncanonical Gβγ signaling pathway that regulates cell-cycle progression. *Dev. Cell* **26**, 358-368. doi:10.1016/j.devcel.2013.07.014

Zaghloul, N. A. and Brugmann, S. A. (2011). The emerging face of primary cilia. *Genesis* **49**, 231-246. doi:10.1002/dvg.20728

Zayzafoon, M. (2006). Calcium/calmodulin signaling controls osteoblast growth and differentiation. *J. Cell. Biochem.* **97**, 56-70. doi:10.1002/jcb.20675

Zhang, Z., Wlodarczyk, B. J., Niederreither, K., Venugopalan, S., Florez, S., Finnell, R. H. and Amendt, B. A. (2011). Fuz regulates craniofacial development through tissue specific responses to signaling factors. *PLoS ONE* **6**, e24608. doi:10.1371/journal.pone.0024608